AD-A039 339 NAVAL POSTGRADUATE SCHOOL MONTEREY CALIF F/G 20/13
NUCLEATE BOILING OF FREON 113 IN THIN LIQUID FILMS.(U)
DEC 76 SOEHANA

UNCLASSIFIED NL

1 OF 1
ADA
039339

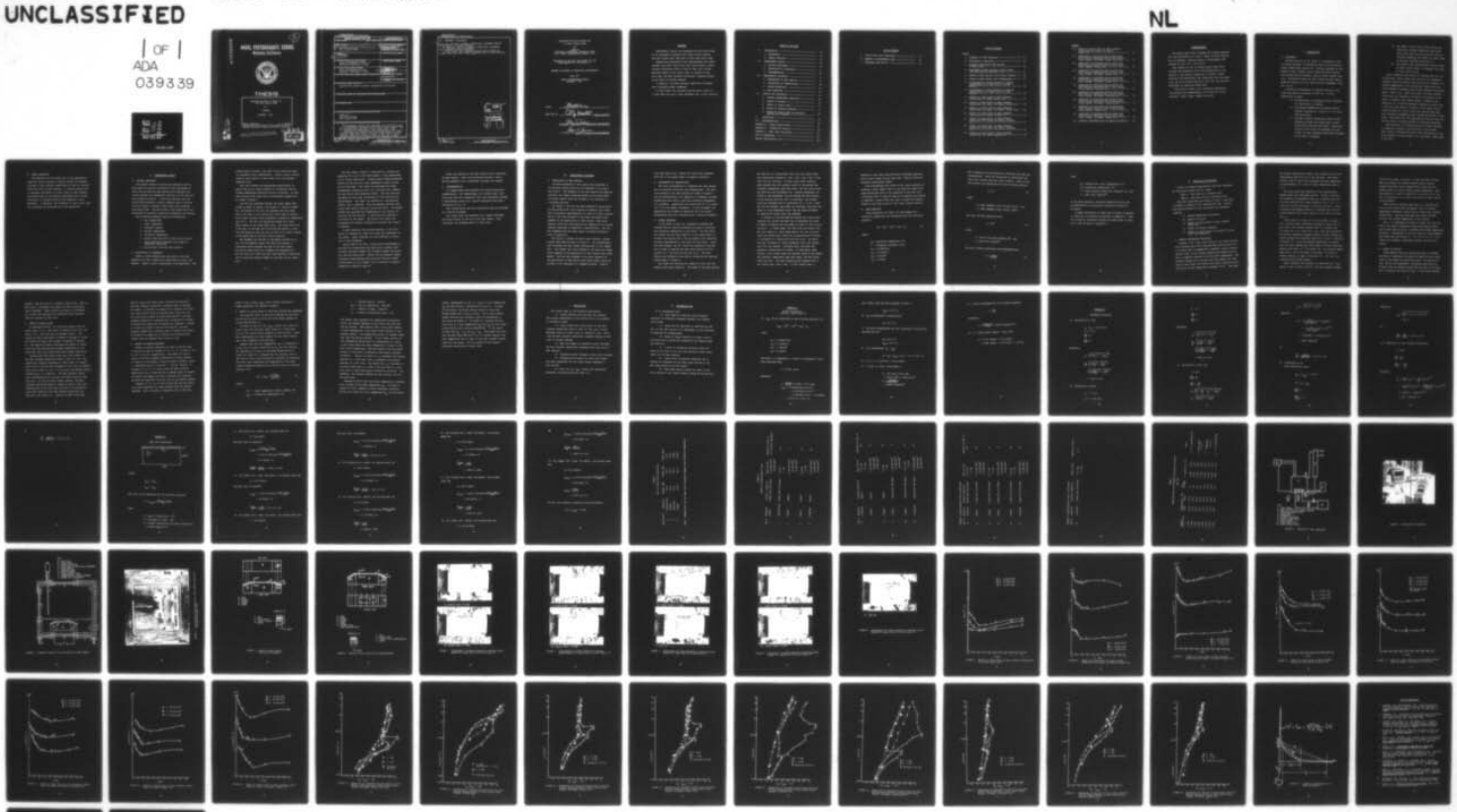

END

DATE
FILMED
5-77

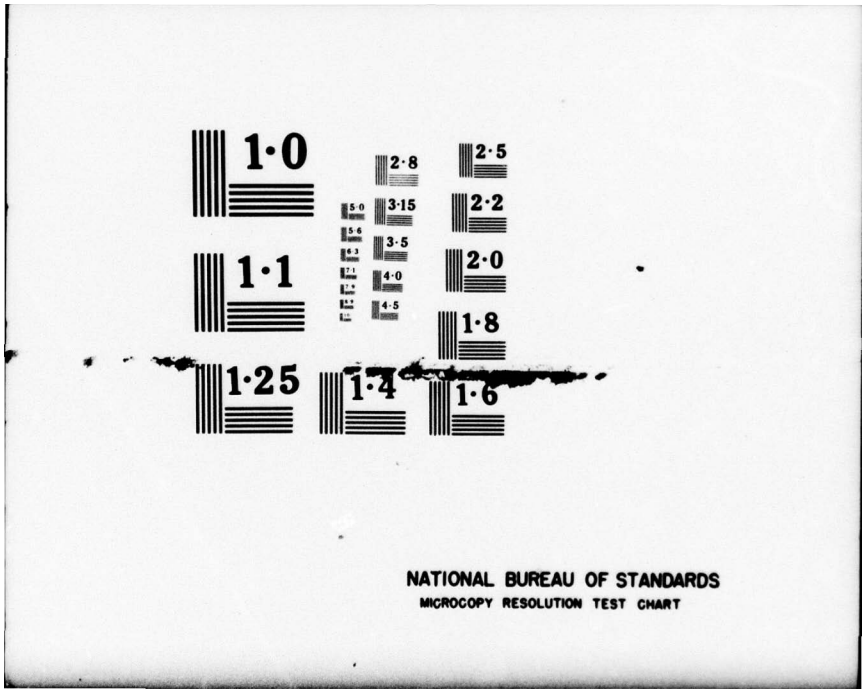
1·0
1·1
1·25
1·4
1·6
1·8
2·0
2·2
2·5
2·8
3·15
3·5
4·0
4·5
5·0
5·6
6·3
NATIONAL BUREAU OF STANDARDS
MICROCOPY RESOLUTION TEST CHART

2

NW

NAVAL POSTGRADUATE SCHOOL
Monterey, California

THESIS

NUCLEATE BOILING OF FREON 113
IN THIN LIQUID FILMS

by

Soehana

December 1976

Thesis Advisor: P. J. Marto

Approved for public release; distribution unlimited.

UNCLASSIFIED

SECURITY CLASSIFICATION OF THIS PAGE (When Data Entered)

REPORT DOCUMENTATION PAGE	READ INSTRUCTIONS BEFORE COMPLETING FORM
1. REPORT NUMBER	2. GOVT ACCESSION NO. 3. RECIPIENT'S CATALOG NUMBER
4. TITLE (and Subtitle) (6) Nucleate Boiling of Freon 113 in Thin Liquid Films.	(9) 5. TYPE OF REPORT & PERIOD COVERED Master's Thesis; December 1976
	6. PERFORMING ORG. REPORT NUMBER
7. AUTHOR(s) (10) Soehana	8. CONTRACT OR GRANT NUMBER(s)
9. PERFORMING ORGANIZATION NAME AND ADDRESS Naval Postgraduate School Monterey, California 93940	10. PROGRAM ELEMENT, PROJECT, TASK AREA & WORK UNIT NUMBERS
11. CONTROLLING OFFICE NAME AND ADDRESS Naval Postgraduate School Monterey, California 93940 (11)	12. REPORT DATE Dec [redacted] 76
	13. NUMBER OF PAGES (12) 83 p.
14. MONITORING AGENCY NAME & ADDRESS(if different from Controlling Office)	15. SECURITY CLASS. (of this report) Unclassified
	15a. DECLASSIFICATION/DOWNGRADING SCHEDULE

16. DISTRIBUTION STATEMENT (of this Report)

Approved for public release; distribution unlimited.

17. DISTRIBUTION STATEMENT (of the abstract entered in Block 20, if different from Report)

18. SUPPLEMENTARY NOTES

19. KEY WORDS (Continue on reverse side if necessary and identify by block number)

Freon 113
Nucleate Boiling
Thin Liquid Film

20. ABSTRACT (Continue on reverse side if necessary and identify by block number)

Experimental results are presented for distilled Freon 113 at atmospheric pressure with liquid levels ranging from pool depths near 10mm down to thin films near 0.2mm.

Temperature measurements with thermocouples and liquid crystals show that liquid level has little effect on heat transfer coefficient above a level of 5mm, and a slight decrease occurs as the liquid level is reduced to 2mm. → next page

DD FORM 1 JAN 73 1473 (Page 1)

EDITION OF 1 NOV 65 IS OBSOLETE S/N 0102-014-6601 |

UNCLASSIFIED

1 SECURITY CLASSIFICATION OF THIS PAGE (When Data Entered)

251450

(20. ABSTRACT Continued)

Below 2mm, the heat transfer coefficient increases sharply as the level is further reduced.

In addition, the heat transfer coefficient increases with increased surface roughness.

In thin films, the incipient boiling point occurs at a lower heat flux and a lower superheat than in pool boiling.

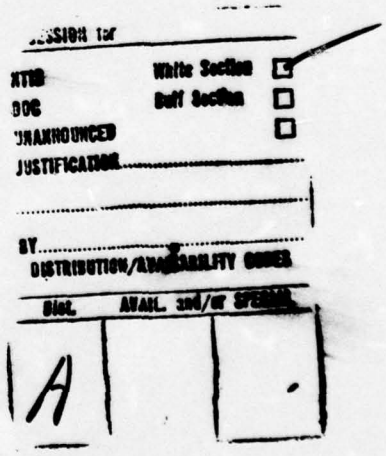

Nucleate Boiling of Freon 113 in Thin Liquid Films

by

Soehana
Lieutenant Commander, Indonesian Navy
B.S., Naval Postgraduate School, 1976

Submitted in partial fulfillment of the
requirements for the degree of

MASTER OF SCIENCE IN MECHANICAL ENGINEERING

from the

NAVAL POSTGRADUATE SCHOOL
December 1976

Author 

Approved by: 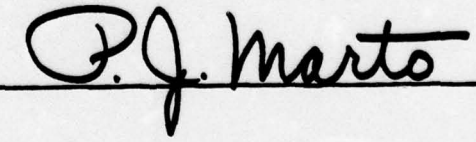
Thesis Advisor

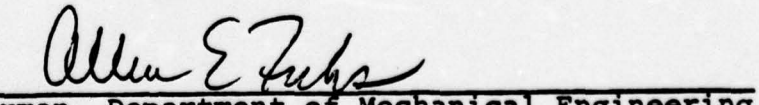
Chairman, Department of Mechanical Engineering

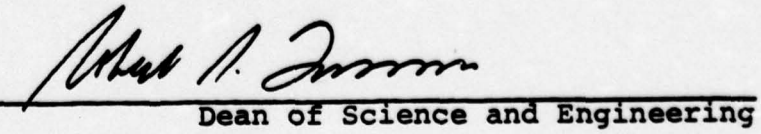
Dean of Science and Engineering

ABSTRACT

Experimental results are presented for distilled Freon 113 at atmospheric pressure with liquid levels ranging from pool depths near 10mm down to thin films near 0.2mm.

Temperature measurements with thermocouples and liquid crystals show that liquid level has little effect on heat transfer coefficient above a level of 5mm, and a slight decrease occurs as the liquid level is reduced to 2mm. Below 2mm, the heat transfer coefficient increases sharply as the level is further reduced.

In addition, the heat transfer coefficient increases with increased surface roughness.

In thin films, the incipient boiling point occurs at a lower heat flux and a lower superheat than in pool boiling.

TABLE OF CONTENTS

LIST OF TABLES

LIST OF FIGURES

Figure

ACKNOWLEDGMENT

The author would like to express his sincere appreciation and gratitude to Dr. Paul J. Marto as thesis advisor for his patience, continual advice, encouragement and interest through this investigation.

Many thanks are due to several people whose help, interest and technical advice contributed much to the success of the project; especially to Messrs. Thomas Christian and James Selby, who constructed the test apparatus, and to my friend Charles R. Ellin for his valuable assistance in typing the rough copy.

I also wish to thank, and I gratefully appreciate, the patience and understanding of my wife Tien and my children: Lindri, Gatot, Mendut and Tiwuk.

I. INTRODUCTION

A. BACKGROUND

Nucleate boiling at low levels is a phenomenon found in various branches of engineering such as the cooling of highly heated metal plates [8]. Another knowledge of this method of heat transfer occurs during two phase annular flow inside boiling channels, such as within nuclear reactors. Nucleation within the thin liquid film may lead to premature break up of the liquid film and subsequent "burn out" [5,13].

A previous investigation of nucleate boiling at low levels was made by Nishikawa in 1966 [8]. In this observation he found:

(1) The population of nucleation sites increases as liquid level is lowered.

(2) The average temperature of heating surface reaches a maximum at a level of 5-7 mm using distilled water.

(3) The heat transfer coefficient remains nearly constant provided the liquid level is maintained above some critical value. Below this critical value (which is different for each liquid) the heat transfer coefficient increases as the level is reduced.

(4) The effect of heat flux on the relation between heat transfer coefficient and liquid level shows that the lower the heat flux is, the more remarkable the effect of liquid level on the heat transfer coefficient is.

(5) The slope of the characteristic boiling curve at lower liquid levels is different from that of usual pool boiling.

Marto, MacKenzie and Rivers [7] observed that for distilled water, ethyl alcohol and Freon 113 at atmospheric pressure, during nucleation boiling from thin heaters, the surface temperature is not uniform and liquid level has little effect on nucleate boiling heat transfer coefficient above a level 5 mm. Below this level, the heat transfer coefficient can increase by as much as 50 percent as the level is reduced, until dryout occurs. Gregor'ev and DudKevich [4] in boiling cryogenic liquids in a thin film, a film which was about 30 microns (0.3 mm) thick, by an atomizing spray of liquid, noted that the critical heat flux increases considerably when liquids are boiled in thin films. They found that the magnitude of critical heat flux and the nature of burnout differ for different materials.

Raad and Myers [9] studied the use of liquid crystals in nucleation studies in pool boiling on thin plates. Their results confirmed the notion that the portion of the plate beneath a growing bubble is a "cold spot" rather than a "hot spot".

B. THESIS OBJECTIVE

The objective of this thesis was to use temperature sensitive liquid crystals to verify further the observed increase in heat transfer coefficient as level is lowered, while heat flux is kept constant. A second objective was to reproduce the effect of liquid level on heat transfer coefficient seen by the previous experiment and to study the effects of surface material and roughness on this phenomena. In addition, the influence of liquid level upon the incipience of nucleation was to be determined.

II. EXPERIMENTAL DESIGN

A. FACTORS CONSIDERED

The overall design of the boiling apparatus used in this study was greatly influenced by the requirement to allow boiling from the test section while mapping with liquid crystals the temperature variation on the test surface caused by boiling. It was also required that the system should maintain a nearly constant mass of boiling fluid to insure a constant liquid level while readings were being taken. The bulk fluid in the system was to be maintained at saturation conditions throughout the testing.

The following parameters were to be determined:

1. Bulk temperature
2. Vapor temperature
3. Barometer reading
4. Ambient temperature
5. Saturation temperature
6. Liquid level relative to the boiling surface
7. Power required to maintain the system at saturation conditions
8. Boiling heat flux from test surface

B. DESCRIPTION OF COMPONENTS

Figure 1 shows schematically the setup of the test apparatus for major testing and identifies all major components. Figure 2 shows a photograph of the apparatus. The

heater shown in Figure 3 was used to boil distilled Freon 113 throughout this investigation. Figure 4 shows a photograph of test section in test vessel with view through removable side.

This test surface was manufactured specifically to permit the use of liquid crystals to investigate boiling surface temperature variations during nucleation. In this case, boiling took place from a rectangularly shaped foil as listed in Table 1.

The foil was stretched between two large copper electrodes as shown in Figure 5 and Figure 6. Prior to assembly, the bottom of the foil was sprayed with flat black paint, and then it was coated with a thin layer of cholesteric liquid crystals which possessed a transition temperature near 59 °C. The foil was sealed and bonded with clear epoxy cement to the large glass block. The glass block was 50 mm long, 25 mm wide, and 26 mm high and served to insulate the bottom of the test foil as well as to permit viewing of the under side of the foil during operation.

The assembly was mounted on adjustable connections to two 6.35 mm diameter copper rods that were mounted in insulating blocks through the side of the test vessel. The entire glass block-foil assembly was suspended in a pool of Freon 113, which was kept near saturation conditions with an auxiliary heater element at the base of the liquid pool.

The test vessel (Figure 3) consisted of a cubical box measuring 203.2 mm on the inside edges; it was constructed of 1/4" thick brass plate. Several glass windows permitted viewing of the test foil from underneath as well as from the top and sides. The vessel was provided with three thermocouple connection ports, an inlet port and a support for the liquid level measuring device. The left side was removable to allow easy interchange of test sections and thermocouples. The vessel was mounted on a cantilevered support from a workbench. This arrangement provided relatively easy viewing from top, bottom and front. The support bracket was provided with thumbscrews at the corners for leveling the test section. A drain was also provided on the bottom of the vessel. The entire test vessel was surrounded with thermal insulation to prevent heat losses to ambient.

A glass condenser was provided external to the test vessel to condense the vapor and return the condensate to the vessel. Tygon condenser line was modified to allow a vent to the atmosphere.

During some of the runs, a quantitative measurement of the test foil temperature was made using a smaller electrically insulated "dummy" foil pressed between the heater foil and the glass block. Three 0.025 mm diameter copper-constantan thermocouples were flattened and spot welded intrinsically to this "dummy" foil to provide an average temperature reading (Figure 6).

Power was supplied to the test section from a regulated DC power supply. Power was controlled through a variac and was measured with a calibrated voltmeter and ammeter.

C. INSTRUMENTATION

All temperatures were measured with copper-constantan thermocouples. The thermocouples for reading vapor, bulk fluid and test foil temperature were read separately through a thermocouple switch and a digital pyrometer which had a resolution of ±0.1 °C.

The voltage across the test section was read and recorded by a digital voltmeter.

The liquid level was measured with a depth micrometer and probe mounted on the top of the test vessel. This instrument was graduated down to 0.0001 inch.

III. EXPERIMENTAL PROCEDURE

A. PREPARATION OF TEST SECTION

The data presented in this report were collected in two separate groups which will be referred to as group A and group B. The assembly of the test section was begun by attaching the copper electrode blocks to the glass block with epoxy cement which was allowed to set overnight in a pressing position.

For group A, the foil was then prepared by spray painting the bottom with a thin coating of Testor's flat black paint followed by approximately 7-8 coats of liquid crystals. The foil was then attached to the glass and copper block assembly by the application of fast drying, clear epoxy cement to both foil and glass and by clamping the two pieces together overnight to establish a complete bond. The foil was roughened with 400 emery paper to promote nucleation prior to operation.

For group B, instead of using liquid crystals, thermocouples were used as shown in Figure 6. The thermocouples were flattened and spot welded intrinsically to the "dummy" foil. The "dummy" foil was attached to the glass and copper block assembly by the application of fast drying clear epoxy cement. The foil was attached to the above assembly by the application of fast drying clear epoxy cement which was allowed to set overnight in a clamped position. Group B

runs were begun with a smooth foil which was roughened with 400 or 320 emergy paper to promote nucleation.

B. CALIBRATION OF THERMOCOUPLES

The first consideration in preparing the test section was to calibrate accurately the thermocouples. The foils were mounted on the test sections as shown in Figure 6, and the thermocouples were immersed in a Rosemont constant temperature bath using a platinum resistance thermometer as a standard. Temperature was raised from 40 °C to about 110 °C in five degree increments. At each increment the temperature was allowed to stabilize for five minutes. Thermocouple data were recorded using a digital pyrometer.

C. NORMAL OPERATION

At the start of each run, atmospheric pressure was recorded from an aneroid barometer and used to calculate the saturation temperature of the Freon. The test fluid was poured into the test vessel to a pool depth about 10 mm above the heating foil, and the heaters were turned on, bringing temperatures to the normal boiling point. Power was then secured, and hot liquid was momentarily drained out in order to measure the zero level position of the liquid (i.e., the level of the test foil). The test section was leveled at this step by adjusting the leveling screws shown in Figure 2.

The vessel was refilled to a depth of 10 mm, and the heaters were again turned on. The power to the test section

was then set to a prescribed value, and the liquid level was successively reduced to 5 mm, 3 mm, 2 mm, 1 mm, 0.5 mm until dry out occurred. At each liquid level setting, after steady state was reached, power to the heaters was recorded, temperature data were taken, and the liquid level was read with the micrometer tip. Because condensate collected on the micrometer tip and because the free surface of the boiling fluid was wavy in character, the average value was recorded with an uncertainty of ± 0.1 mm. After dry out was reached, the vessel was refilled, the power was reset to a new prescribed value, and the above procedure of varying the liquid level was repeated.

A variety of runs was made by holding the liquid level constant and varying the heat flux to determine the onset of bubble nucleation and the effect of level on this incipient point. In these cases, the test fluid was poured into the test vessel to a pool depth about 8 mm, and the power input was varied from 2 Watts up to approximately 50 Watts in increments of 2 Watts until boiling began. The power was then increased in 5 Watt increments until the highest heat flux was reached. Following this, the power was gradually reduced back to 2 Watts. At each power level setting, after steady state was reached, power to the heater was recorded, temperature data were taken, and the liquid level was read. The above operation was repeated with a low liquid level (near 1 mm). In this latter case, a

decrease in the level occurred during prolonged operation due to vapor losses out the vent hole. Make-up fluid was therefore occasionally added.

Color photographs were taken of the liquid crystals by focusing a Nikon camera with a 55 mm lens with Kodak high speed Ektachrome film on the underside of the test foil. A Colortran 3200 °K lamp was used to illuminate the surface. In addition a glass filter was used to reduce the heating effect of the light source on the liquid crystal surface.

D. DATA REDUCTION

Using properties for Freon 113 from Chapman [2], saturation temperature was determined from the following equation:

$$T_S = A_1P^3 + A_2P^2 + A_3P + A_4 \qquad (1)$$

where:

T_S = saturation temperature (°F)
P = atmospheric pressure (psia)
A_1 = 0.0018971518
A_2 = -0.17542512
A_3 = 7.6127221
A_4 = 37.42493

Wall temperature was determined by averaging the read out thermocouples. Level was determined by subtracting the zero level reading from each level reading. Power to the test section was determined from the following equation:

$$Q = VI \tag{2}$$

where

V = test assembly input voltage (Volts), and
I = test assembly input current (Amps).

The heat flux was determined from

$$q = Q/A \tag{3}$$

where

A = area of the test surface (m^2), and
q = heat flux ($Watt/m^2$).

The heat transfer coefficient was determined from

$$h = \frac{q}{(T_W - T_S)} \tag{4}$$

where

T_W = average wall (foil) temperature (°C)

T_S = saturation temperature (°C)

h = heat transfer coefficient (Watts/m^2 °C), and

q = heat flux (Watts/m^2).

In the above equation, corrected temperatures were used as determined by the previously mentioned calibration procedure.

A sample calculation of these data is given in Appendix A, along with an uncertainty analysis in Appendix B. Heat loss caused by conduction through the glass block is about 1.3% - 4.85% as shown in Appendix C.

IV. RESULTS AND DISCUSSION

A total of eighteen experimental runs were completed. All runs were grouped into two types:

Type A: vary level at a constant flux

Type B: vary heat flux at a constant level.

Test foil conditions are listed in Table 1, and Table 2 presents a summary of all experimental runs. Results have been divided into five categories for discussion purposes:

(1) Surface temperature variations

(2) Aspect of boiling

(3) Effect of liquid level on heat transfer coefficient

(4) Effect of surface roughness

(5) Effect of liquid level on incipient boiling point and hysterisis.

A. SURFACE TEMPERATURE VARIATIONS

Figures 5 and 6 show color prints of the liquid crystal color patterns which were observed when boiling Freon 113. It is known that as temperature increases, liquid crystals reflect light in the visible spectrum and change color at what is commonly referred to as the event temperature. The crystals change from colorless and first appear red, then yellow, then green, and finally blue before becoming colorless again as the temperature increases [3,11]. Note that

the coldest temperatures appear black because of the black undercoating applied prior to the crystals. The liquid crystals used in this study possessed an event temperature of approximately 59 °C with an event temperature span of 3 °C.

The prints show the underside of the rectangularly shaped heater foil described earlier. Figure 7 contains the sequence of photographs taken at a constant heat flux of 30,000 Watts/m^2 with liquid levels of 10.4, 4.5, 1.2, 0.68 and 0.35 mm and finally at the dry out point. Figure 8 contains the sequence taken at a constant heat flux of 20,000 Watts/m^2 with liquid levels of 0.41 and 0.2 mm and dry out.

Notice that at a level of 10.4 mm as seen in Figure 7(a), during natural convection, because of the motion of the liquid, the crystals change color in a gradual way. In Figure 7(b), at a level of 4.5 mm, with less convection, the surface temperature appears almost uniform, because the liquid crystals are uniformly deep blue in color. Therefore in Figure 7(b), since the surface temperature is greater than the event temperature (which means a surface superheat greater than about 13 °C for Freon 113), the crystals appear deep blue in color and sharp at the edge. As level is further reduced, as shown in Figures 7(c), 7(d) and 7(e), irregular dark patches appear.

These irregular dark patches are identified as a cold region, since in their vicinity, the color rapidly changes

from blue to green, to yellow, to red, and then to black. The cold patches are evident because several closely grouped nucleation sites commulatively cooled the foil surface below the liquid crystal event temperature. This same behavior is seen in Figure 8(a) at a level of 0.4 mm and in Figure 8(b) at a level of 0.2 mm for a heat flux at 20,000 Watts/m^2.

These results therefore show that at a constant heat flux, as the liquid level decreases, the foil surface temperature decreases, giving rise to larger heat transfer coefficients. The data also show that during nucleate boiling, the surface temperature is not uniform.

The dry out phenomena are shown in Figure 7(f) and 8(c). Notice the larger irregularly shaped blue regions which have closely spaced colors, indicating very sharp temperature gradients. Evaporation of the thin layer of liquid between the wetted area and the dry out area causes the cool areas around this boundary, indicated by green, red and black colors.

B. ASPECT OF BOILING

Since bubbles form from nucleating sites, an attempt was made to investigate the effect of heat flux and liquid level on the number of nucleation sites. As a matter of fact, during this experiment, nucleating sites were not evident since the bubbles formed from the edge of the test foil, disturbing the field of view. It was quite evident,

however, from the runs at a constant liquid level, that as heat flux is increased, the number of active nucleating sites increased. These results are similar to Nikishawa [8] in that the population of nucleation sites increase with the increase of heat flux.

C. EFFECT OF LIQUID LEVEL

As mentioned earlier, all runs were grouped into two types, type A (i.e., vary level at constant heat flux) and type B (i.e., vary heat flux at constant level). The results of type A are shown in Figures 9 through 16, while the results of type B can be seen in Figures 17 through 25. The results of type A runs show the effect of liquid level upon the boiling heat transfer coefficient of all three test foils with smooth and rough surface conditions.

Results show that liquid level has little effect on the heat transfer coefficient above a level of 5 mm. The coefficient slightly decreases as liquid level is lowered from 5 mm to 2 mm and then increases as the level is reduced from 2 mm to about 0.2 mm. At this level the surface usually reached the dry out condition. The heat transfer coefficient increases more at low heat flux rather than at high heat flux. At very low heat fluxes, however, the heat transfer coefficient shows an opposite trend to that just described due to the fact that only one or two nucleation sites were evident on the test surface during this low heat flux (see Figure 11). Results of type A runs show

that at a heat flux level about 30,000-36,000 Watts/m^2, the heat transfer coefficient increases about 38 percent for Nickel, 29 percent for Copper and 37 percent for Titanium, while liquid level was reduced from 2 mm to 0.2 mm. At a heat flux of about 20,000-25,000 Watts/m^2, the heat transfer coefficient increases about 39 percent for Nickel, 40 percent for Copper and 39 percent for Titanium. Finally at a heat flux about 15,000-16,000 Watts/m^2, the heat transfer coefficient increases about 52 percent for Nickel, 50 percent for Copper and 70 percent for Titanium while liquid level was reduced from 2 mm to 0.2 mm.

D. EFFECT OF SURFACE ROUGHNESS

Effect of surface roughness for type A runs and type B runs can be seen in Figures 10, 11, 13, 14, 16 and 17, 19, 20, 22, 23 and 25, respectively. The effect of liquid level on the heat transfer coefficient of rough surfaces is similar to the effect of level on smooth surfaces, which is described earlier in Section C. Notice, however, in Figures 10, 11, 13, 14, and 16 that the heat transfer coefficient with a rough surface increases about 80 percent for Nickel and Copper and about 25 percent for Titanium at about the same heat flux over that of the smooth surface.

Figures 17, 19, 20, 22 and 25 show that boiling occurs at a lower superheat for rough surfaces than for smooth surfaces. This is similar to Rohsenow [10] in that the

slope of the q VS($T_W - T_{sat}$) curve rotates clockwise to higher superheats for smoother surfaces.

E. EFFECT OF LIQUID LEVEL ON INCIPIENT BOILING AND HYSTERESIS

The incipient point of boiling is defined as the point on the boiling curve at which the first bubble appears on the boiling surface [1].

As shown in the q VS ($T_W - T_{sat}$) curves, as a result of type B runs, the incipient point occurs at a lower heat flux for low liquid levels compared to pool boiling. Lower wall temperatures are also evident for low liquid levels, near 1 mm, compared to pool boiling.

Suppose that the wall temperature, T_W, is referred to as T_{W_1} for low liquid levels and as T_{W_2} for pool boiling. The inception of boiling is indicated schematically in Figure 26, where it is assumed that two cavities (size A and size B) exist on the surface for purposes of discussion. The solid curve represents the temperature of the vapor inside nucleating bubbles and is derived from the following equation [12]:

$$T_v^* = T_{sat} + \frac{2 \sigma T_{sat}}{h_{fg} \rho_v r_c} \qquad (5)$$

where:

T_v^* = vapor temperature inside a bubble (°F)

T_{sat} = saturation temperature (°F)

σ = surface tension [lbf/ft]

h_{fg} = heat of evaporation [BTU/lbm]

ρ_v = density of vapor [lbm/ft^3]

r_c = radius of nucleating cavity [ft]

The dashed lines represent the temperature distribution within the thermal sublayer of the liquid very near the boiling surface. When heating from a flat plate surface, a highly superheated liquid region forms adjacent to the heating surface. The temperature profile is assumed linear very near the heating surface. If the linear portion of this temperature distribution is extrapolated to a point in the liquid where the local temperature is equal to the bulk liquid temperature, then the distance from the heater surface to this point is defined as the thermal sublayer thickness δ. Notice in Figure 26, δ_2 represents the laminar sublayer in a thick pool, and δ_1 represents the laminar sublayer in a thin film. The reason why δ_1 is sketched in as being larger than δ_2 is due to the fact that in a thin film there is much less natural convection occurring. Consequently, the laminar sublayer can grow further out into the bulk fluid.

Nucleation occurs when the liquid temperature is greater than or equal to the vapor temperature T_v*. As shown in Figure 26, with a bubble of size A available, incipient boiling will occur at a wall temperature T_{w_1} for low liquid

levels, represented as line (1), and at a wall temperature T_{W_2} for pool boiling, represented as line (2). It means at low levels, incipient boiling occurs at lower heat fluxes rather than in pool boiling. For a rough surface, larger cavities are available, which is represented in the figure by bubble B. For bubble B, incipient boiling will occur at a wall temperature T_{W_1}' and T_{W_2}' for low liquid levels and for pool boiling respectively. It can easily be seen that $T_{W_1}' < T_{W_1}$ and $T_{W_2}' < T_{W_2}$. This means that with more and more large cavities (i.e., a rougher surface) the wall temperature will be less, so the heat transfer coefficient will be larger. This is similar to the results previously described for type B runs.

V. CONCLUSIONS

This study leads to the following conclusions:

(1) During nucleate boiling from thin heaters, the surface temperature is not uniform due to the presence of nucleation sites.

(2) Liquid level has little effect on the heat transfer coefficient above a level of 5 mm, and a slight decrease occurs as liquid level is reduced to 2 mm. Below 2 mm the heat transfer coefficient increases sharply as the level is further reduced.

(3) When the number of nucleation sites increases, the heat transfer coefficient increases while heat flux is kept constant.

(4) Nucleation sites increase as heat flux increases.

(5) Nucleate boiling begins at lower heat fluxes and lower superheats for low liquid levels compared to pool boiling.

(6) The q VS $(T_W - T_{sat})$ curves show substantial hysteresis characteristics for Freon 113.

VI. RECOMMENDATIONS

It is recommended that:

(1) This study be continued using different materials of different roughness together with several test fluids.

(2) Great care be exercised in handling the test foil on the test section with improvement in the technique of applying the thermocouples.

(3) Epoxy be chosen carefully in order to get a good bond and to reduce the trapping of air bubbles under the test foil.

(4) A fluid in saturation condition should be ready at any time to fill the test section so that liquid levels can be kept constant.

(5) Liquid level be measured carefully due to forming of condensate at the level probe and due to the wavy characteristics of the liquid.

(6) High speed motion pictures be taken of the color changes of the liquid crystals caused by the boiling.

APPENDIX A

SAMPLE CALCULATION
(Run #11, Data Point #1)

a) T_{sat} can be determined by the following equation [2]:

$$T_{sat} = A_1P^3 + A_2P^2 + A_3P + A_4$$

where

$$A_1 = 0.0018971518$$
$$A_2 = -0.17542512$$
$$A_3 = 7.6127221$$
$$A_4 = 37.424943$$

and where T is expressed in °F and P is expressed in psia. From tabulated data,

$$P = 29.88 \text{ mm Hg}$$

therefore

$$P = \frac{29.88}{29.92} \times 14.696 = 14.67 \text{ psia}$$

$$T_{sat} = (0.0018971518)(14.67)^3 - (0.17542512)(14.67)^2 + (7.6127221)(14.67) + 37.424943$$

$$= 117.34 \text{ °F} = 47.4 \text{ °C.}$$

As a check, from the data recorded in Table 3,

$$T_{sat} = 47.2\ °C.$$

b) T_W is determined by reading data:

$$T_W = 65.4\ °C,$$

c) The above temperatures are then corrected by calibration outlined earlier:

$$T_W = 65.2\ °C$$
$$T_{sat} = 47.0\ °C.$$

d) ΔT is determined, $T_W - T_{sat}$:

$$\Delta T = T_W - T_{sat} = 65.2 - 47.0 = 18.2\ °C.$$

e) $Q = V \cdot I = (1.508)(34) = 51.272$ Watts

f) $q = Q/A$, A = area. From Table 1,

$$A = (55.6\ mm) \times (25.4\ mm)$$
$$= 1412.24\ mm^2 = 0.00141224\ m^2$$
$$q = \frac{51.272}{0.00141224}$$
$$= 36305.44\ Watts/m^2$$

g) h can be determined by the following equation:

$$h = \frac{q}{\Delta T}$$

therefore:

$$h = \frac{36,305.44}{18.2} = 1994.80 \text{ Watts/m}^2 \text{ °C}$$

h) H = liquid level reading - zero level

H = 1.703 inches - 1.413 inches

= 0.290 inches = (0.29)(25.4) = 7.36 mm

APPENDIX B

UNCERTAINTY ANALYSIS

(a) Uncertainty in area

$$\omega_L = \omega_W = \pm 0.05 \text{ inch}$$

$$A = L \times W$$

$$\frac{\partial A}{\partial L} = W$$

$$\frac{\partial A}{\partial W} = L$$

Therefore,

$$\omega_A = \sqrt{(W\omega_L)^2 + (L\omega_W)^2}$$

$$\frac{\omega_A}{A} = \sqrt{(\frac{\omega_L}{L})^2 + (\frac{\omega_W}{W})^2}$$

$$= \sqrt{(\frac{.05}{2.625})^2 + (\frac{.05}{1})^2}$$

$$= .054 \text{ or } 5.4\%$$

(b) Uncertainty in power

$$\omega_I = \pm .25 \text{ A}$$

$$\omega_V = \pm .005 \text{ volt}$$

$$Q = VI$$

$$\frac{\partial Q}{\partial V} = I$$

$$\frac{\partial Q}{\partial I} = V$$

Therefore,

$$\omega_Q = \sqrt{(I\omega_V)^2 + (V\omega_I)^2}$$

$$\frac{\omega_Q}{Q} = \sqrt{(\frac{\omega_V}{V})^2 + (\frac{\omega_I}{I})^2}$$

$$= \sqrt{(\frac{.005}{1.508})^2 + (\frac{.25}{34})^2}$$

$$= .0081 \text{ or } 0.81\%$$

(c) Uncertainty in heat flux

$$q = Q/A$$

$$\frac{\partial q}{\partial Q} = \frac{1}{A}$$

$$\frac{\partial q}{\partial A} = -\frac{Q}{A^2}$$

$$\omega_q = \sqrt{(-\frac{Q}{A^2} \cdot \omega_A)^2 + (\frac{1}{A}\omega_Q)^2}$$

$$\omega_A = \sqrt{(W\omega_L)^2 + (L\omega_W)^2}$$

$$\omega_Q = \sqrt{(I\omega_V)^2 + (V\omega_I)^2}$$

Therefore,

$$\omega_q = \left[\left(\frac{51.27}{.0013306425^2}\right)^2 (.000093)^2 + \left(\frac{1}{.0013306425^2}\right)^2 (1.5)^2\right]^{1/2}$$

$$= [(7252385.0 + 1270748.8)]^{1/2}$$

$$= 2919.4 \text{ Watts/m}^2$$

or

$$\frac{\omega_q}{q} = \frac{2919.4}{38530.25} = .076 \text{ or } 7.6\%$$

(d) Uncertainty in ΔT

From calibration curve:

$$\omega_{T_W} = \omega_{T_{sat}} = \pm 0.2 \text{ °C}$$

$$\Delta T = T_W - T_{sat}$$

$$\frac{\partial \Delta T}{\partial T_W} = 1$$

$$\frac{\partial \Delta T}{\partial T_{sat}} = -1$$

Therefore,

$$\omega_{\Delta T} = \sqrt{(1)^2(.2)^2 + (-1)^2(.2)^2}$$

$$= .28\ ^\circ C$$

or

$$\frac{\omega_{\Delta T}}{\Delta T} = \frac{.28}{18.2} = .015 \text{ or } 1.5\%$$

(e) Uncertainty in heat transfer coefficient

$$h = q/\Delta T$$

$$\frac{\partial h}{\partial q} = \frac{1}{\Delta T}$$

$$\frac{\partial h}{\partial \Delta T} = -\frac{q}{\Delta T^2}$$

Therefore,

$$\omega_h = \left[\left(\frac{1}{\Delta T}\right)^2(\omega_q)^2 + \left(\frac{q}{\Delta T^2}\right)^2(\omega_T)^2\right]^{1/2}$$

$$= \left[\left(\frac{1}{18.2}\right)^2(2919.4)^2 + \left(\frac{38561.76}{(18.2)^2}\right)^2(.28)^2\right]^{1/2}$$

$$= [(25607.0 + 1060.88)]^{1/2}$$

$$= 163.3 \text{ Watts/m}^2\ ^\circ C$$

or

$$\frac{\omega_h}{h} = \frac{163.3}{2117.13} = .077 \text{ or } 7.7\%$$

APPENDIX C

HEAT LOSS CALCULATION

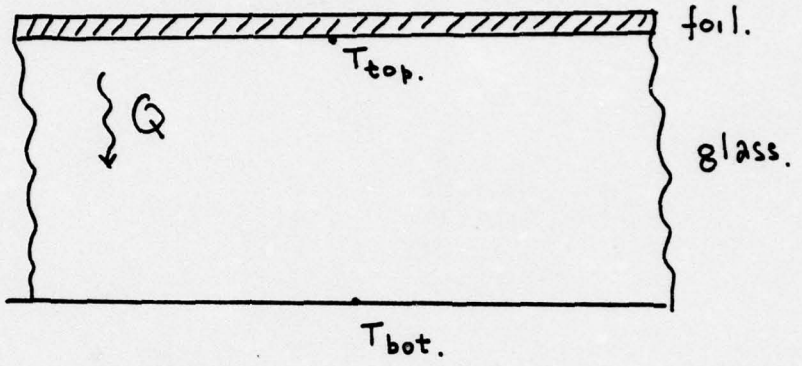

Assume

$$T_{top} \simeq T_{foil}$$

$$T_{bot} \simeq T_{liq}$$

Heat loss can be determined by the following equation:

$$Q = k_{glass}\, A\left[\frac{T_{foil} - T_{liq}}{\Delta x}\right]$$

where

A = area of glass block (m^2)

Δx = thickness of glass (mm)

k = thermal conductivity of glass (Watt/cm °C)

= 0.0109 (Watt/cm °C)

(1) for Nickel foil, smooth, the maximum power was

$$Q = 48.42 \text{ Watt}$$

The heat loss is therefore:

$$Q_{loss} = kA\left[\frac{T_{foil} - T_{liq}}{\Delta x}\right]$$

$$= (1.09)(0.00134112)\left[\frac{75.6 - 47.6}{.026}\right]$$

$$= 1.57 \text{ Watts, or}$$

$$\frac{Q_{loss}}{Q} = \frac{1.57}{48.42} = .0325 \text{ or } 3.25\%$$

(2) For Nickel foil, rough (400 emery), the maximum power was

$$Q = 39.43 \text{ Watts}$$

The heat loss is therefore

$$Q_{loss} = (1.09)(0.00134112)\left[\frac{58 - 47.4}{.026}\right]$$

$$= .59 \text{ Watts, or}$$

$$\frac{Q_{loss}}{Q} = \frac{.59}{39.41} = .015 \text{ or } 1.5\%.$$

(3) For Nickel foil, rough (320 emery), the maximum power was

$$Q = 49.8 \text{ Watts.}$$

The heat loss is therefore

$$Q_{loss} = (1.09)(0.00134112)\left[\frac{59.2 - 47.4}{.026}\right]$$

$$= .66 \text{ Watts, or}$$

$$\frac{Q_{loss}}{Q} = \frac{0.66}{49.8} = 0.013 \text{ or } 1.3\%.$$

(4) For Titanium foil, smooth, the maximum power was

$$Q = 49.27 \text{ Watts}$$

$$Q_{loss} = (1.09)(0.00141224)\left[\frac{66.8 - 47.8}{.026}\right]$$

$$= 1.12 \text{ Watts, or}$$

$$\frac{Q_{loss}}{Q} = \frac{1.12}{49.27} = .023 \text{ or } 2.3\%.$$

(5) For Titanium foil, smooth, the minimum power was

$$Q = 20.2 \text{ Watts}$$

$$Q_{loss} = (1.09)(0.00141224)\left[\frac{65.4 - 48.4}{.026}\right]$$

$$= 1.01 \text{ Watts, or}$$

$$\frac{Q_{loss}}{Q} = \frac{1.01}{20.2}$$

$$= .0498 \text{ or } 4.98\%$$

(6) For Titanium foil, rough (400 emery), the minimum power was

$$Q = 20.25 \text{ Watts}$$

$$Q_{loss} = (1.09)(0.00141224)\left[\frac{65.2 - 48.6}{.026}\right]$$

$$= .98 \text{ Watts, or}$$

$$\frac{Q_{loss}}{Q} = \frac{.98}{20.25}$$

$$= .0485 \text{ or } 4.85\%.$$

(7) For Titanium foil, rough (320 emery), the minimum power was

$$Q = 20.17 \text{ Watts}$$

$$Q_{loss} = (1.09)(0.00141224)\left[\frac{61.8 - 48.2}{.026}\right]$$

$$= .805 \text{ Watts, or}$$

$$\frac{Q_{loss}}{Q} = \frac{.805}{20.17}$$

$$= .0399 \text{ or } 3.99\%.$$

(8) For copper foil, smooth, the minimum power was

$$Q = 21.164 \text{ Watts}$$

$$Q_{loss} = (1.09)(0.00141224)\left[\frac{64.2 - 48.2}{.026}\right]$$

$$= .947 \text{ Watts, or}$$

$$\frac{Q_{loss}}{Q} = \frac{.95}{21.164}$$

$$= .0447 \text{ or } 4.47\%.$$

(9) For copper foil, rough (320 emery), the minimum power was

$$Q = 21.37 \text{ Watts}$$

$$Q_{loss} = (1.09)(0.00141224)\left[\frac{57.8 - 48.2}{.026}\right]$$

$$= 0.58 \text{ Watts, or}$$

$$Q_{loss} = \frac{0.58}{21.37}$$

$$= 0.027 \text{ or } 2.7\%.$$

So heat loss caused by conduction can be bracketed:

$$1.3\% < Q_{loss} < 4.85\%$$

TABLE 1

List of Test Foil Conditions

Test Foil #	Material	Length (mm)	Width (mm)	Thick (mm)
1	Nickel-Iron	50.8	25.4	0.03
2	Nickel	52.8	25.4	0.03
3	Titanium	55.6	25.4	0.051
4	Copper	52.38	25.4	0.013

Note: Lengths are not the same since aluminum clamps have different dimensions.

TABLE 2

Summary of Experimental Runs

Run #	Material	Surface Condition	Type of Run	Results in Fig. #
1	Nickel	Rough with 400 emery	A 30,000 W/m^2	5,6 (liquid crystals)
			20,000 W/m^2	
2	Nickel-Iron	Rough with 320 emery	B 9 mm	15
			1 mm	
3	Nickel	Smooth	A 30,000 W/m^2	7
			21,000 W/m^2	
			15,000 W/m^2	
4	Nickel	Smooth	B 10 mm	16
			0.9 mm	
5	Titanium	Smooth	A 35,000 W/m^2	10
			24,000 W/m^2	
			14,000 W/m^2	

Run #	Material	Surface Condition	Type of Run	Results in Fig. #
6	Titanium	Smooth	B 8.3 mm	19
			1.1 mm	
7	Copper	Smooth	A 35,000 W/m^2	13
			25,000 W/m^2	
			16,000 W/m^2	
8	Copper	Smooth	B 9 mm	22
			1 mm	
9	Nickel	Rough with 400 emery	A 30,000 W/m^2	8
			19,500 W/m^2	
			8,000 W/m^2	
10	Nickel	Rough with 400 emery	A 10.5 mm	17
			1.5 mm	
11	Titanium	Rough with 400 emery	A 36,000 W/m^2	11
			24,000 W/m^2	
			14,000 W/m^2	

Summary of Experimental Runs (Continued)

Run #	Material	Surface Condition	Type of Run	Results in Fig. #
12	Titanium	Rough with 400 emery	B 7.5 mm	20
			1.2 mm	
13	Copper	Rough with 320 emery	A 35,000 W/m^2	14
			25,000 W/m^2	
			16,000 W/m^2	
14	Copper	Rough with 320 emery	B 9 mm	23
			1.3 mm	
15	Nickel	Rough with 320 emery	A 30,000 W/m^2	9
			20,000 W/m^2	
			6,000 W/m^2	
16	Nickel	Rough with 320 emery	B 10 mm	18
			1.3 mm	
17	Titanium	Rough with 320 emery	A 34,000 W/m^2	12
			23,000 W/m^2	
			14,000 W/m^2	

Summary of Experimental Runs (Continued)

Run #	Material	Surface Condition	Type of Run	Results in Fig. #
18	Titanium	Rough with 320 emery	B 8.5 mm	21
			1.1 mm	

TABLE 3

Tabulated Data for Sample Calculation Purpose

Run #11

Liquid Level (in)	Temperature (°C) T_{sat}	T_{wall}	Power A (amp)	V (volts)	ΔT (°C)	Note
1.730	47.2	65.4	34	1.508	18.2	1. A = 0.00141224 m^2
1.690	47.2	65.6	34	1.500	18.4	
1.623	47.2	65.8	34	1.506	18.6	2. zero level
1.535	47.2	66.0	34	1.506	18.8	= 1.413"
1.465	47.2	64.8	34.5	1.511	17.6	3. $T_{(ambient)}$
1.433	47.2	63.6	34.5	1.515	16.4	= 66 °F
1.426	47.2	62.6	34.5	1.521	15.4	
1.416	47.2	62.2	34	1.509	15.0	4. P = 29.88 mm Hg

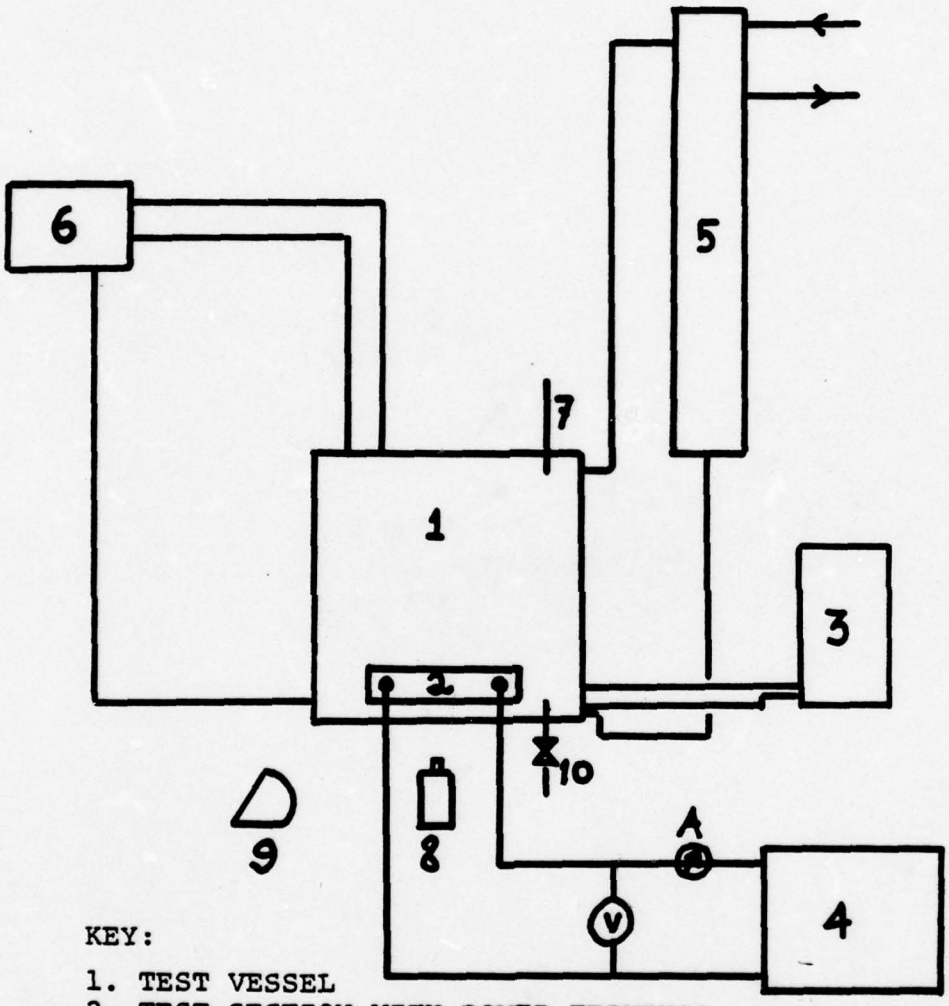

KEY:

1. TEST VESSEL
2. TEST SECTION WITH POWER TERMINAL
3. AUXILIARY POWER SUPPLY
4. POWER SUPPLY
5. CONDENSER
6. DIGITAL PYROMETER
7. LIQUID LEVEL PROBE
8. NIKON CAMERA
9. COLOR TRAN LIGHT
10. VESSEL DRAIN VALVE

FIGURE 1. Schematic of Test Apparatus

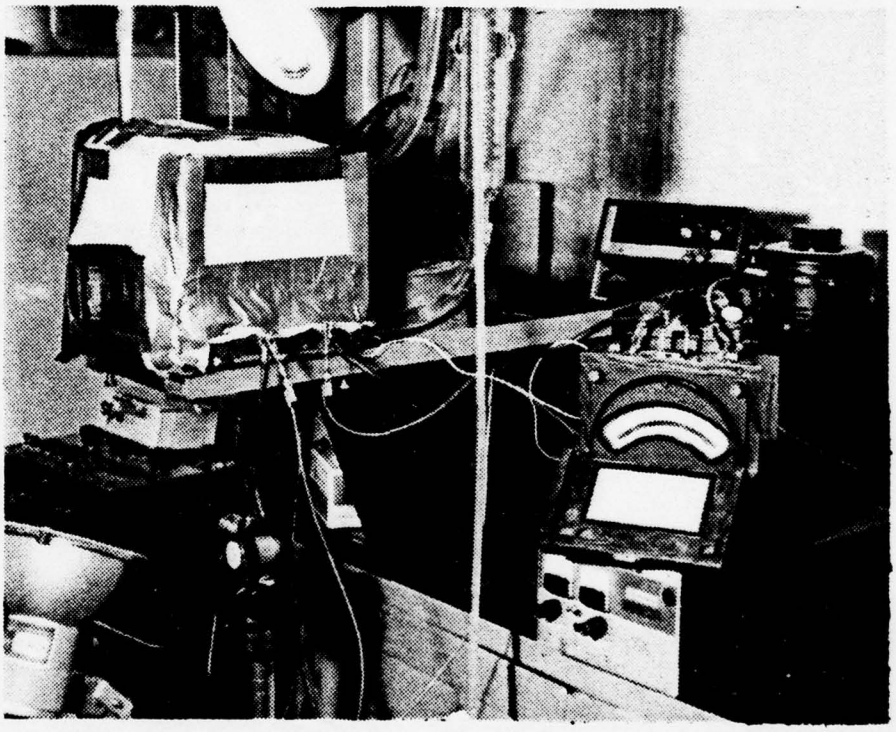

FIGURE 2. Photograph of Apparatus

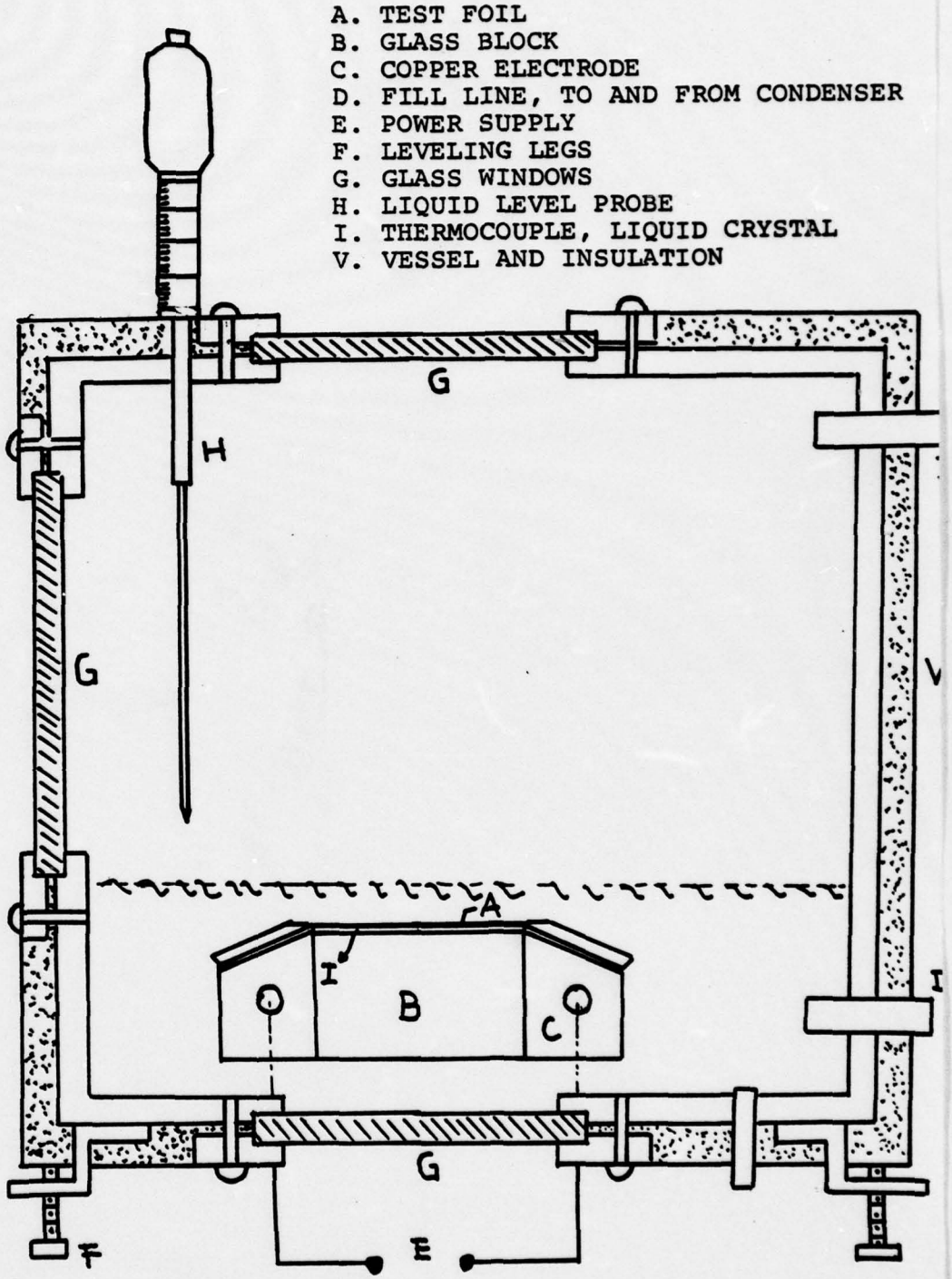

FIGURE 3. Schematic Drawing of Test Section in Test Vessel

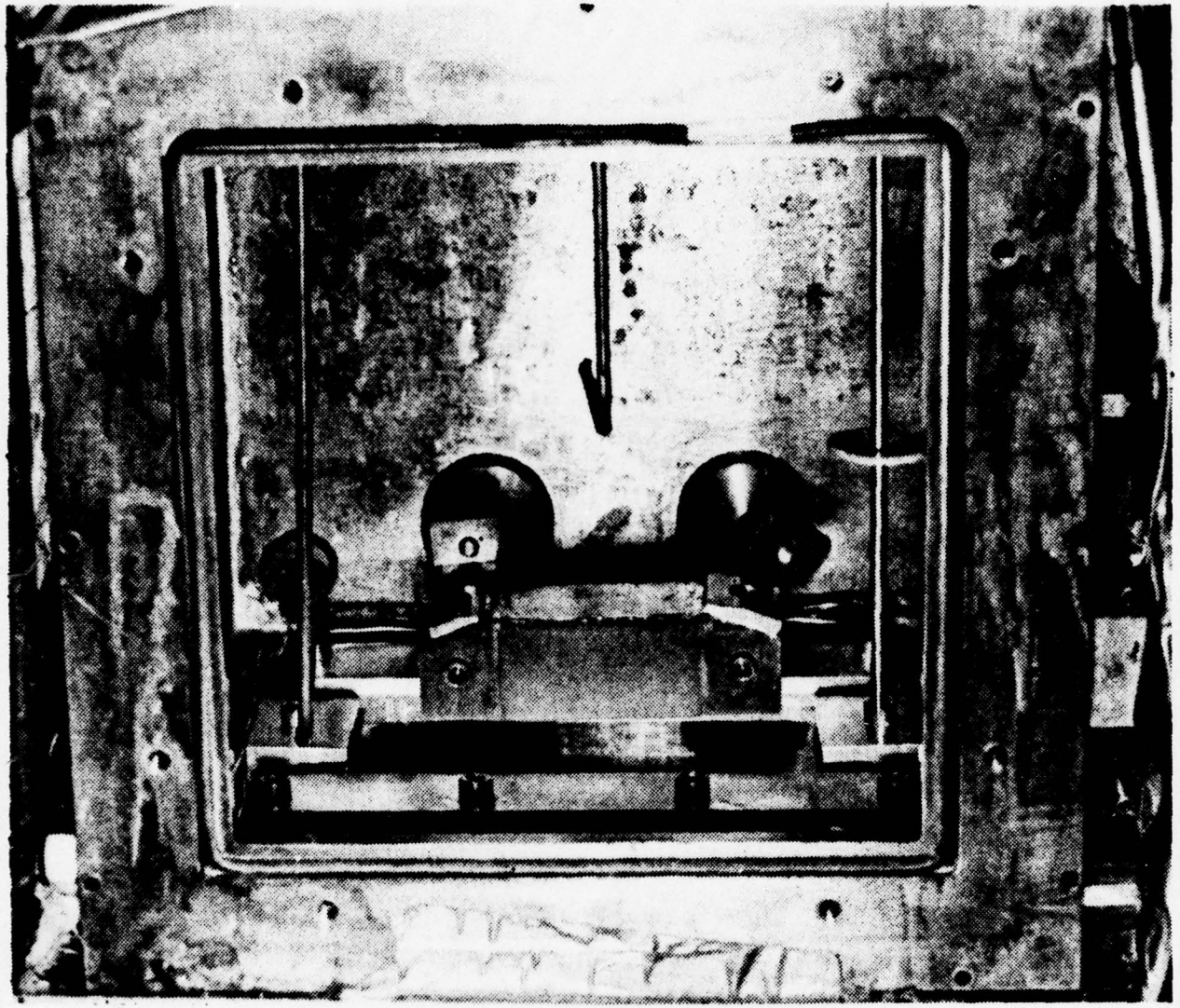

FIGURE 4. Photograph of Test Section in Test Vessel with View Through Removable Side

TOP VIEW

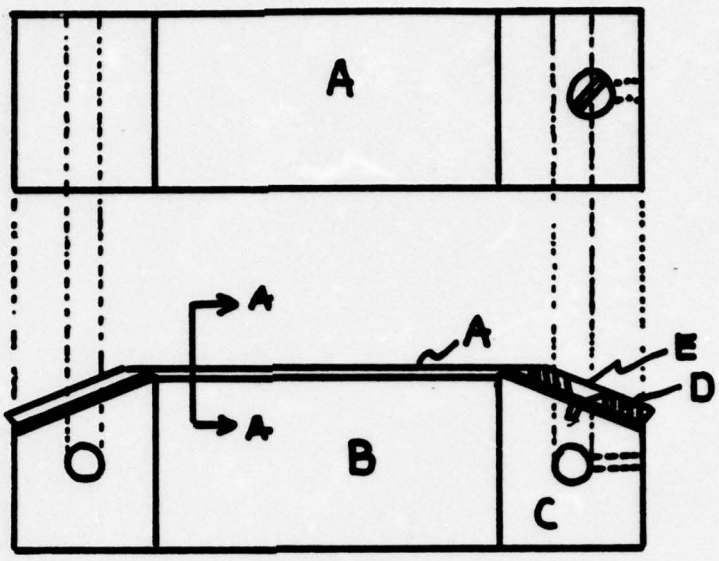

SIDE VIEW

A. FOIL
B. GLASS
C. COPPER
D. CLAMP
E. SCREW

SECTION A-A

1. foil
2. black paint
3. liquid crystal
4. epoxy

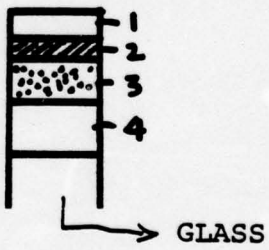

FIGURE 5. Sketch of Test Section with Liquid Crystals

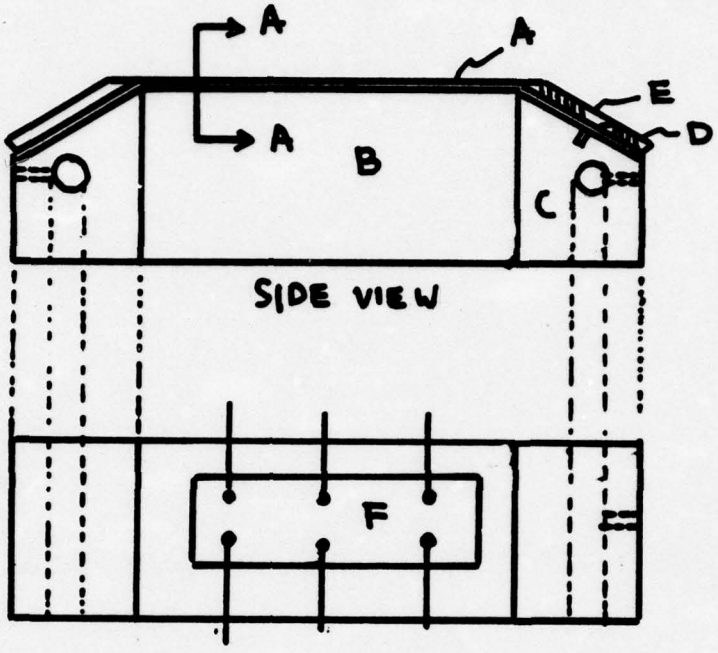

A. FOIL
B. GLASS
C. COPPER
D. CLAMP
E. SCREW
F. "DUMMY" FOIL
WITH THERMOCOUPLES

SECTION A-A

1. foil
2. black paint
3. "dummy" with thermocouple
4. epoxy

FIGURE 6. Sketch of Test Section with Thermocouples

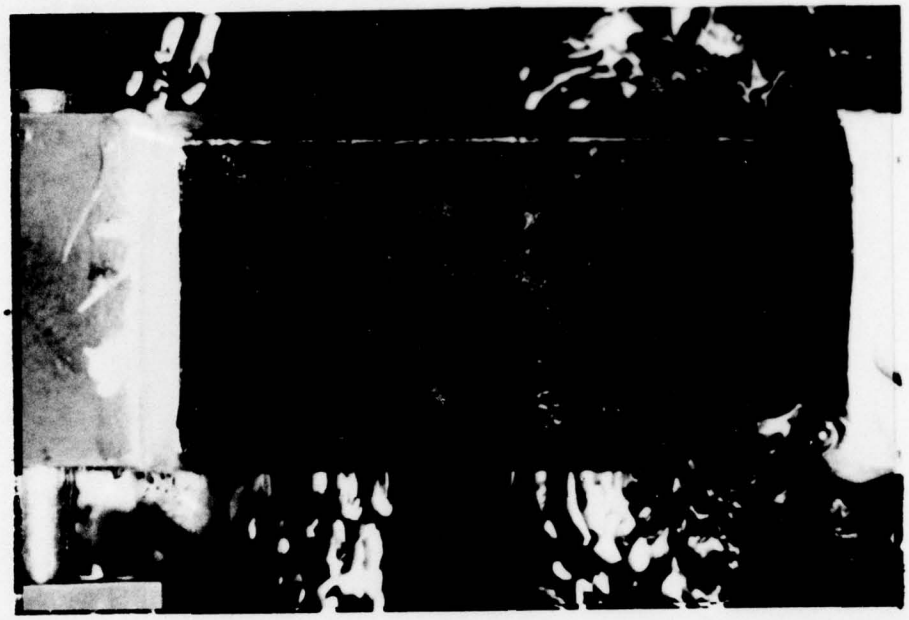

(a) liquid level =10.4mm

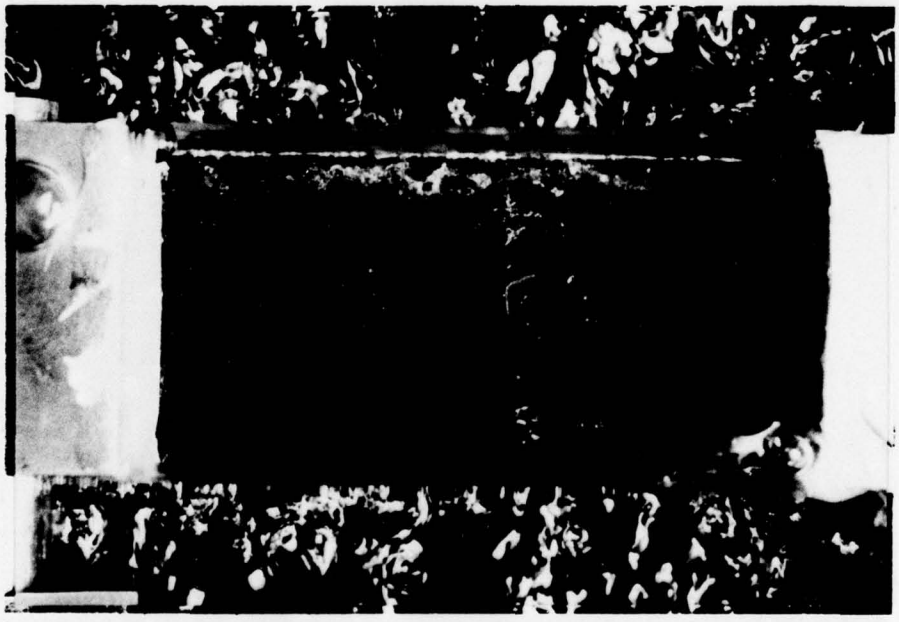

(b) liquid level = 4.5mm

FIGURE 7. Photographs of Liquid Crystals at Varying Liquid Levels at a Heat Flux of 30,000 Watts/m^2

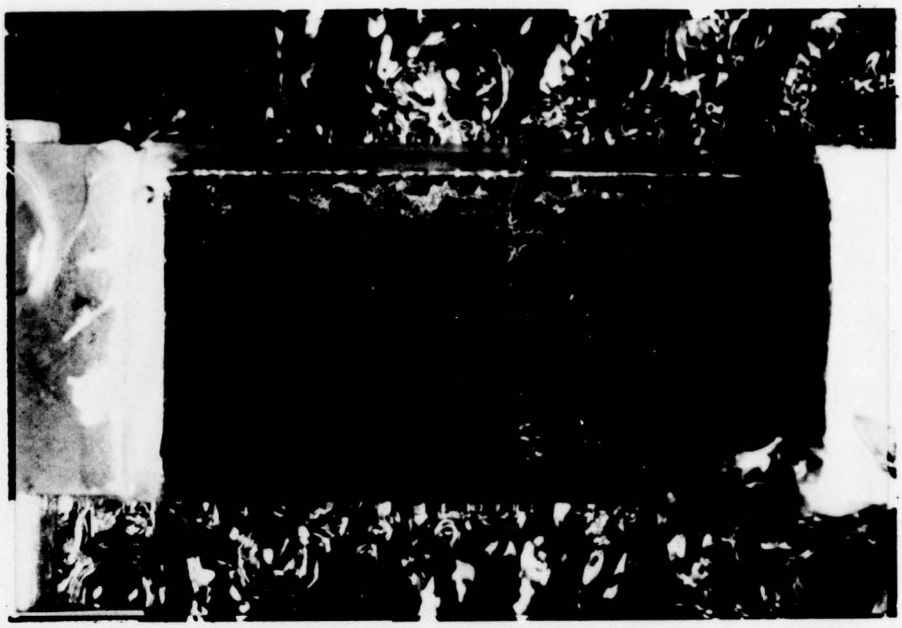

(c) liquid level = 1.2mm

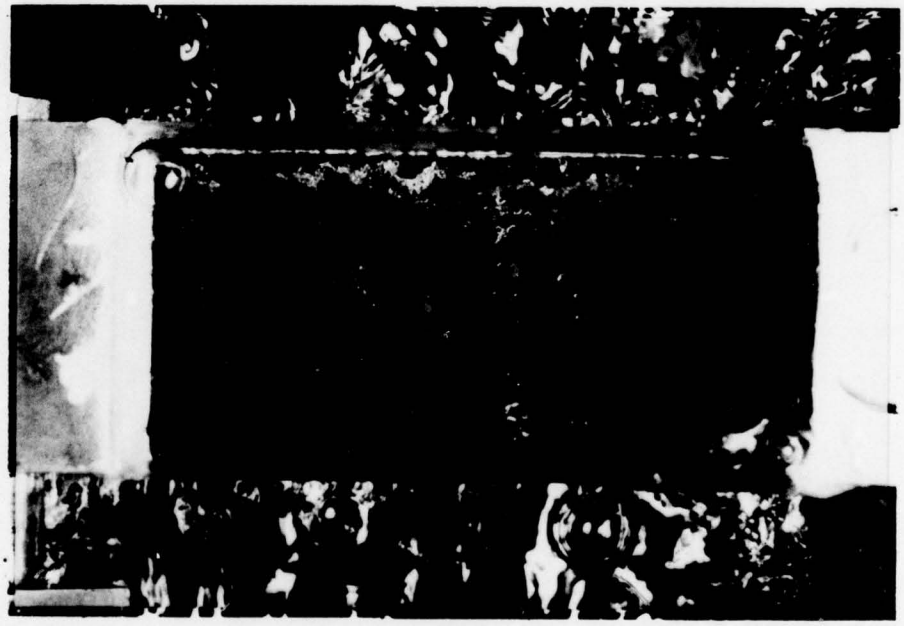

(d) liquid level = 0.68mm

FIGURE 7. Photographs of Liquid Crystals at Varying Liquid Levels at a Heat Flux of 30,000 Watts/ m^2

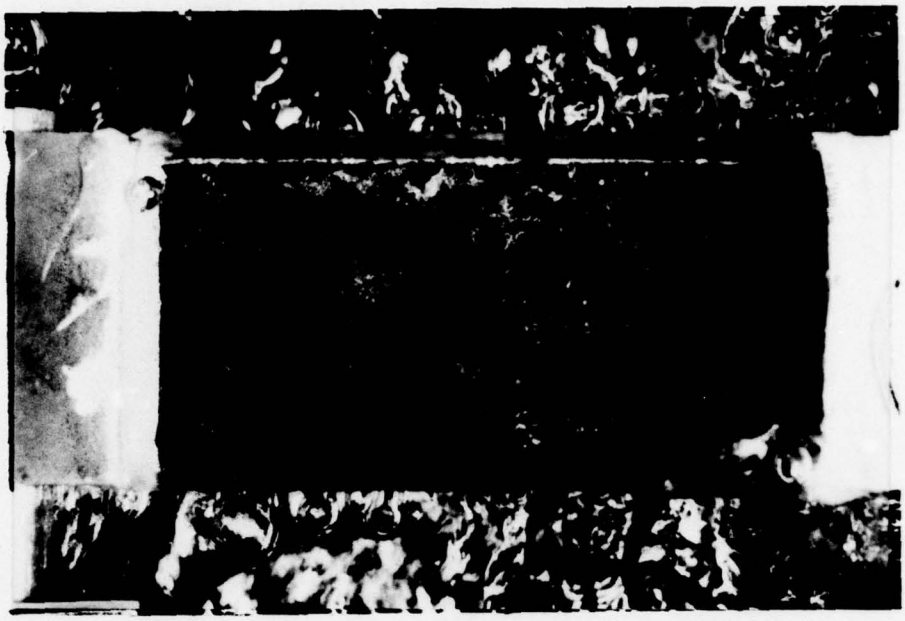

(e) liquid level = 0.35mm

(f) dry out

FIGURE 7. Photographs of Liquid Crystals at Varying Liquid Levels at a Heat Flux of 30,000 Watts/ m^2

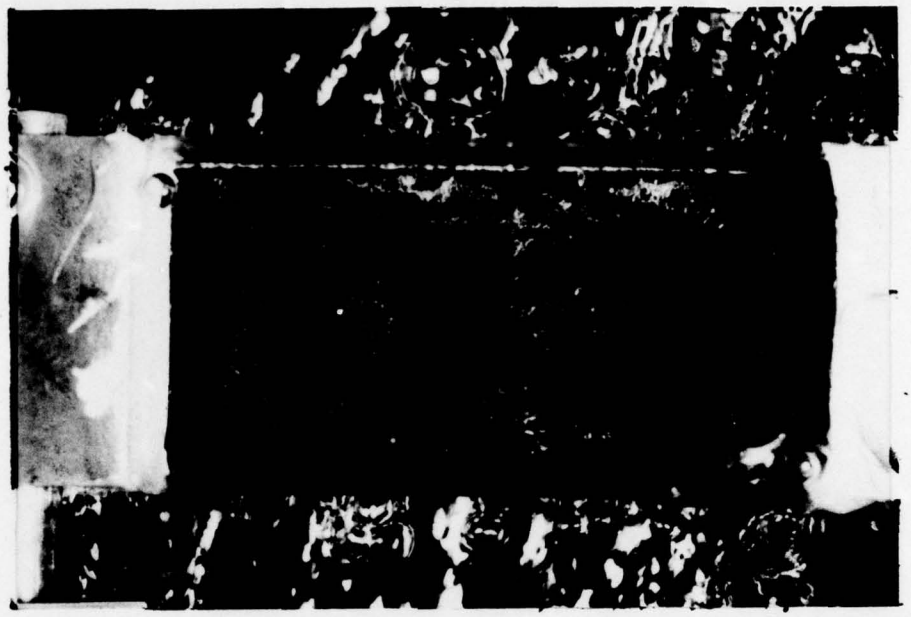

(a) liquid level = 0.41mm

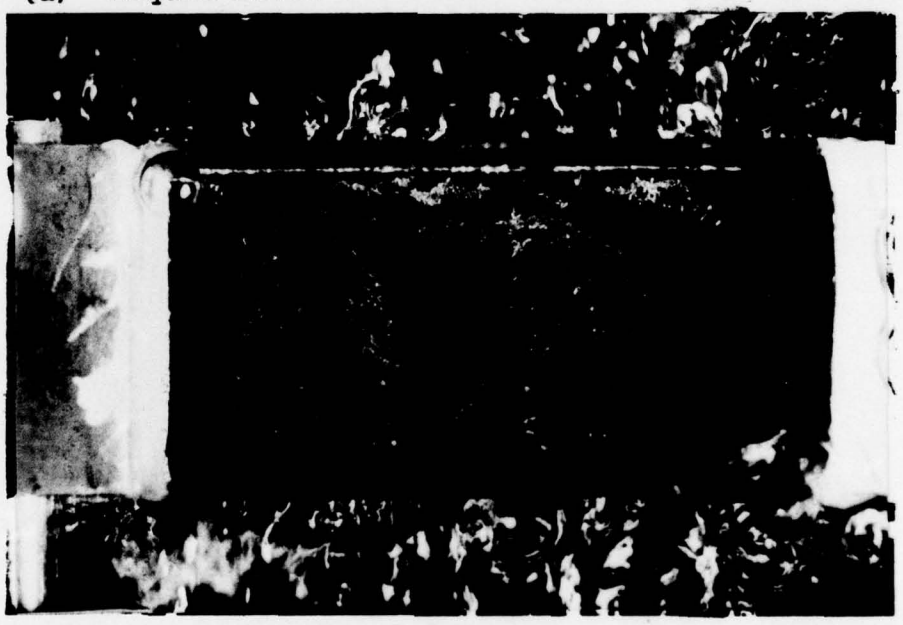

(b) liquid level = 0.2mm

FIGURE 8. Photograph of Liquid Crystals at Varying Liquid Levels at a Heat Flux of 20,000 Watts/ m^2

(c) dry out

FIGURE 8. Photographs of Liquid Crystals at Varying Liquid Levels at a Heat Flux of 20,000 Watts/ m^2

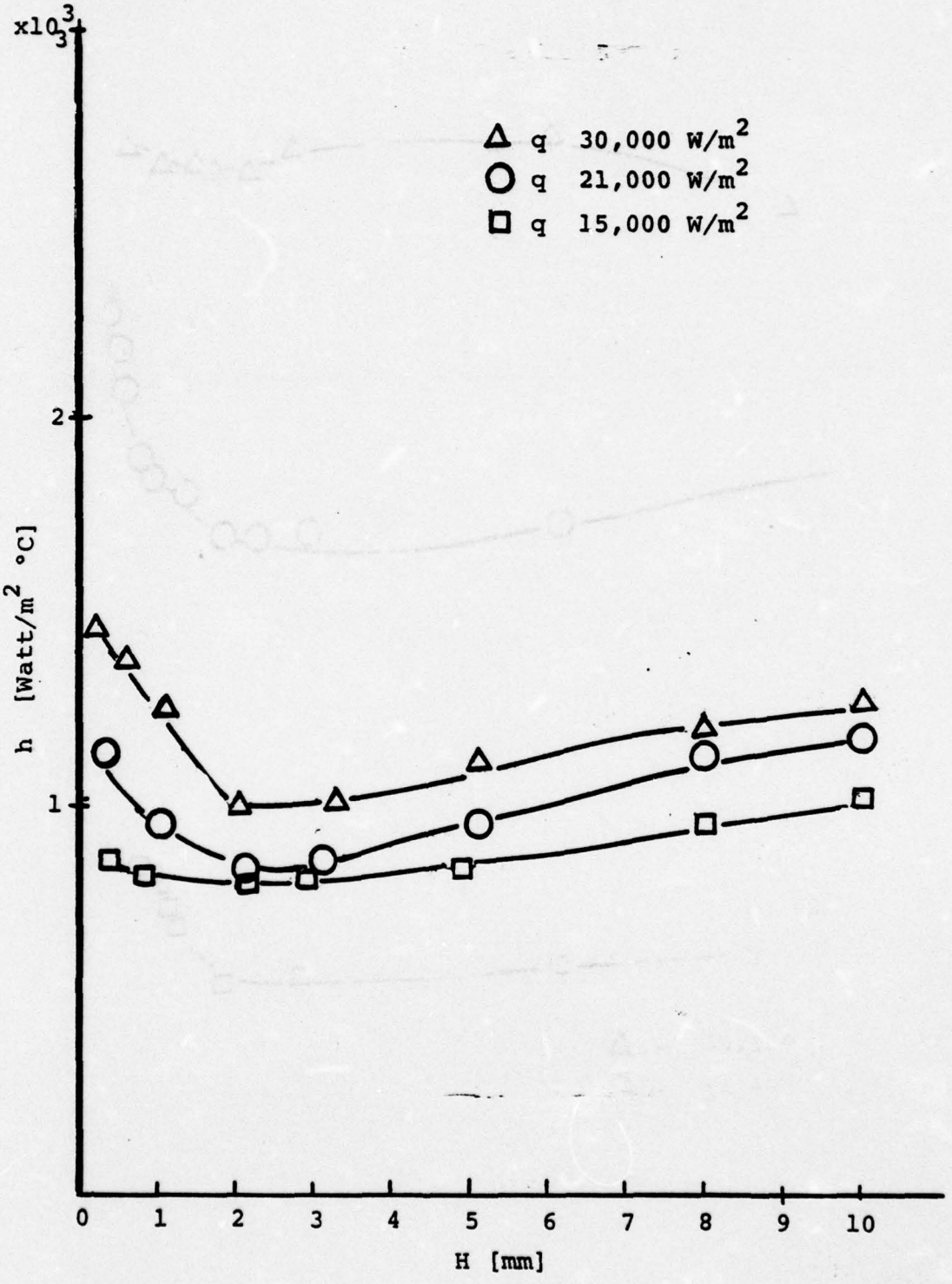

FIGURE 9. Effect of Liquid Level on Heat Transfer Coefficient for Smooth Nickel Foil

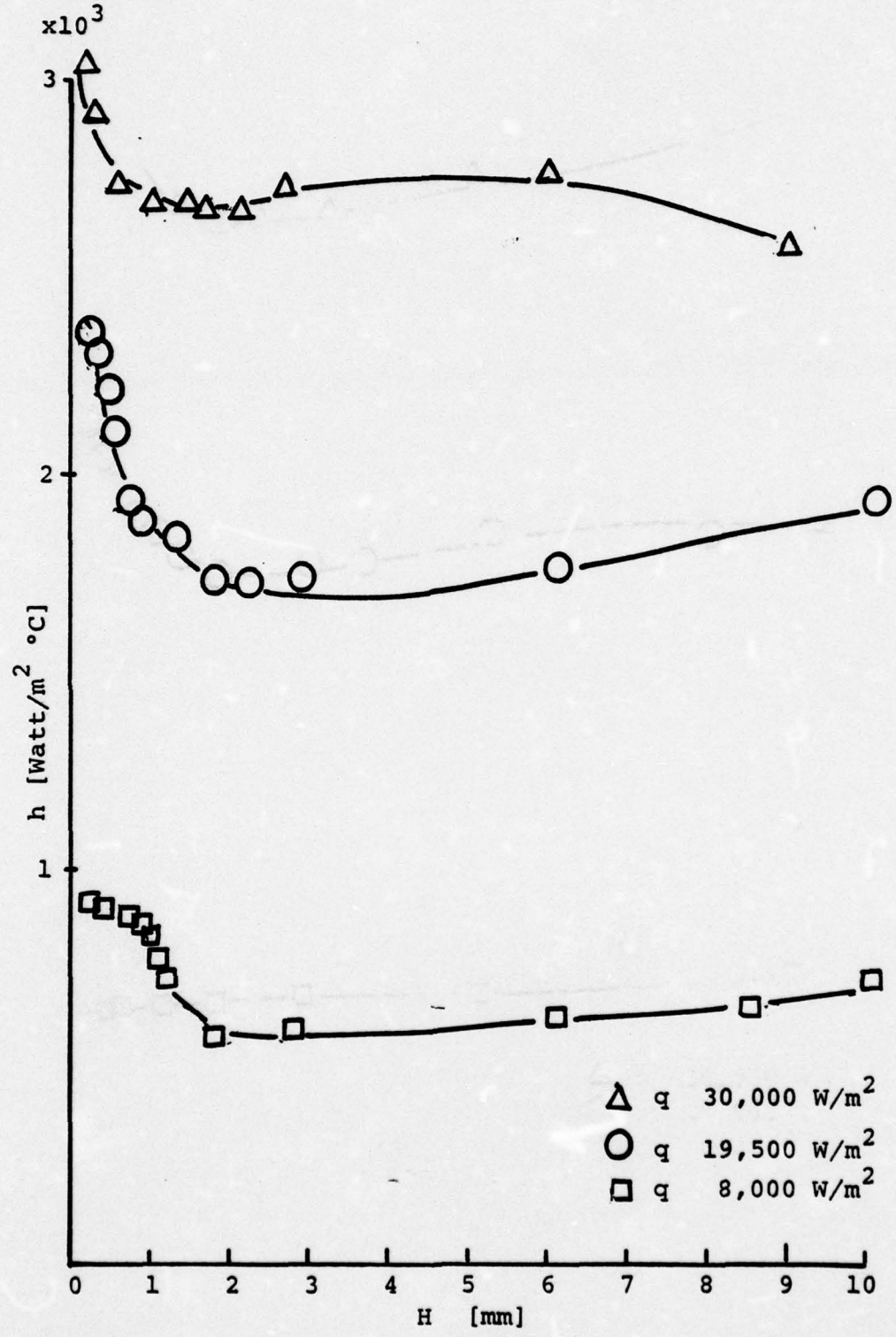

FIGURE 10. Effect of Liquid Level on Heat Transfer Coefficient for Rough (400 Emery) Nickel Foil

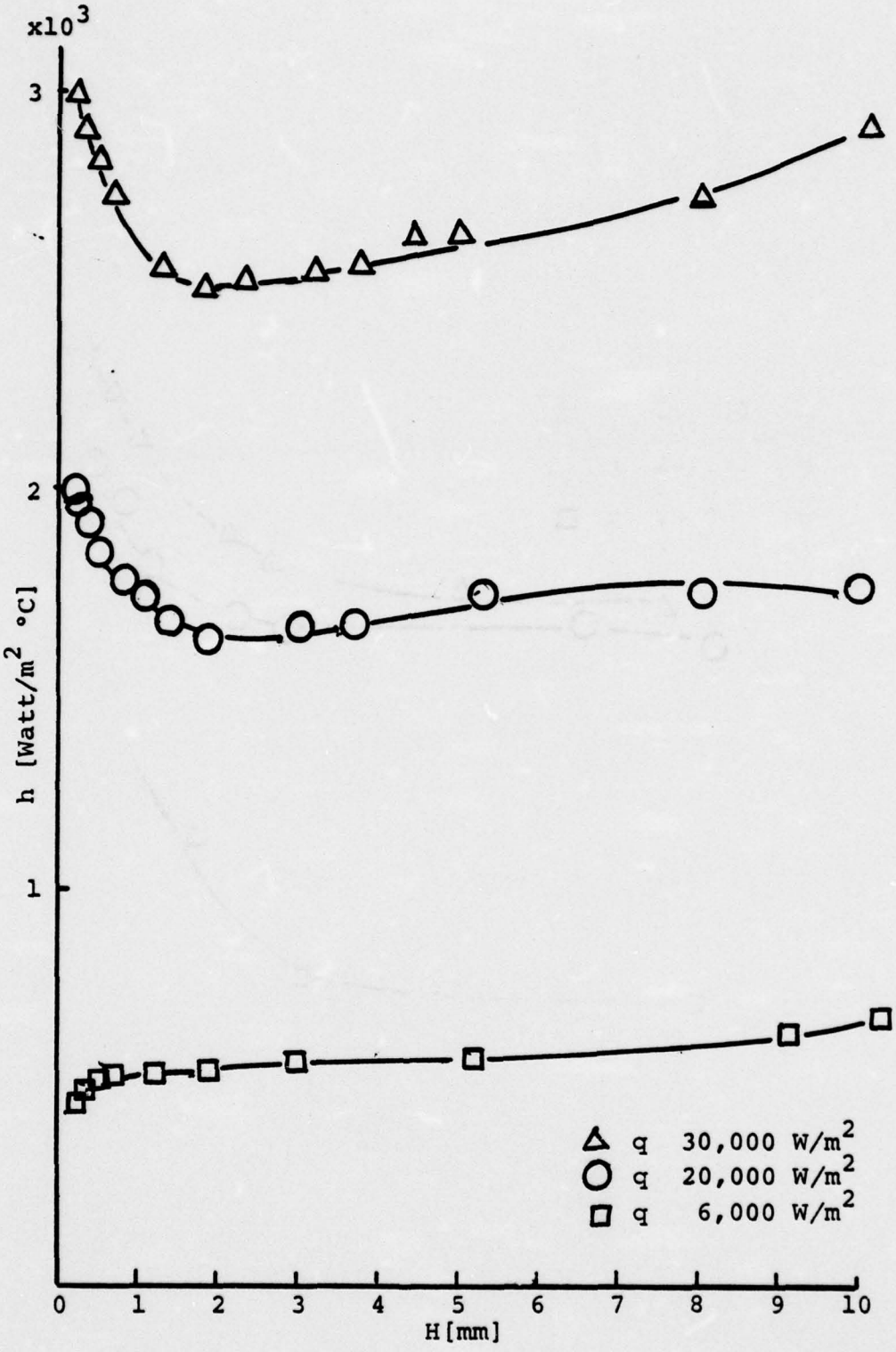

FIGURE 11. Effect of Liquid Level on Heat Transfer Coefficient for Rough (320 Emery) Nickel Foil

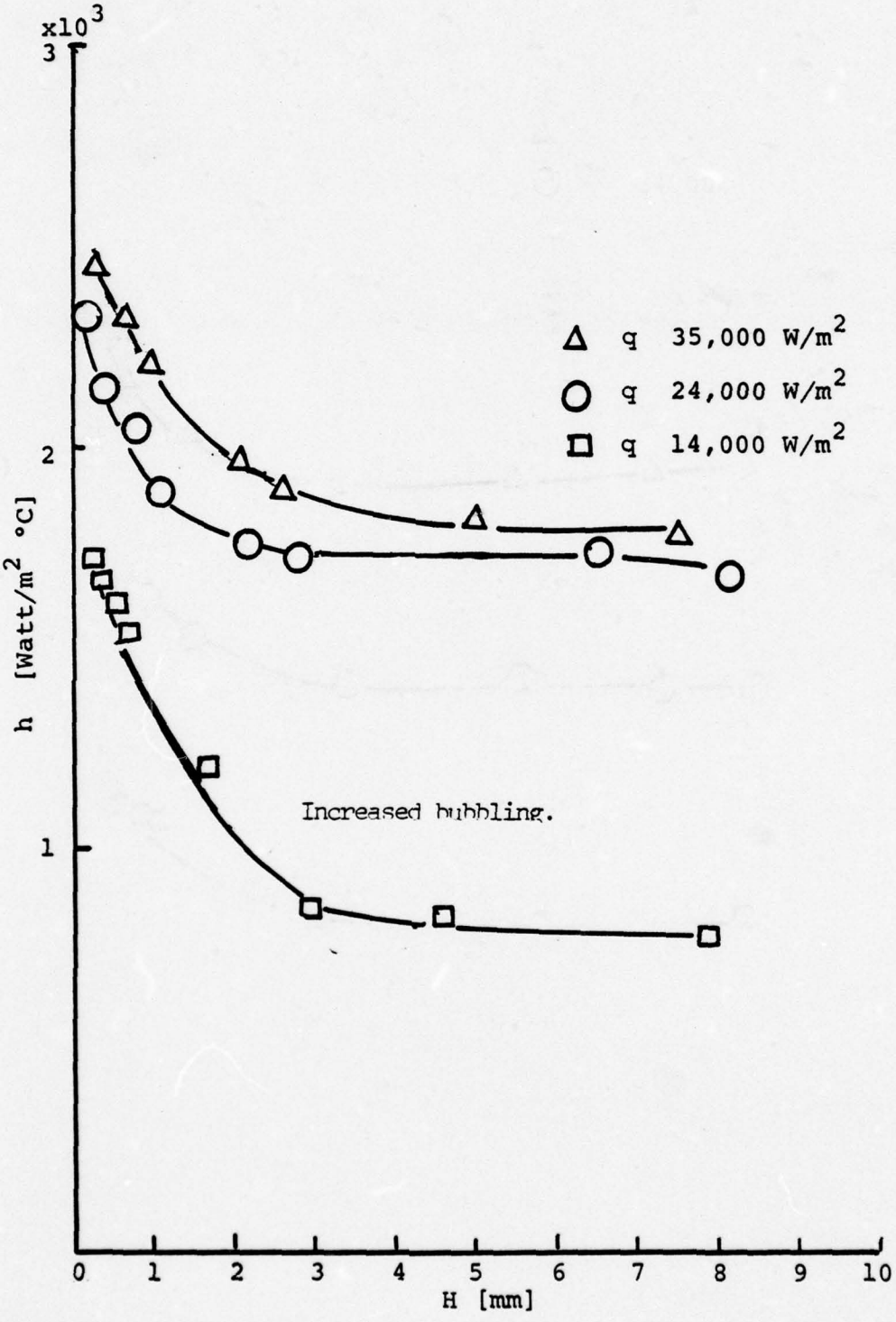

FIGURE 12. Effect of Liquid Level on Heat Transfer Coefficient for Smooth Titanium Foil

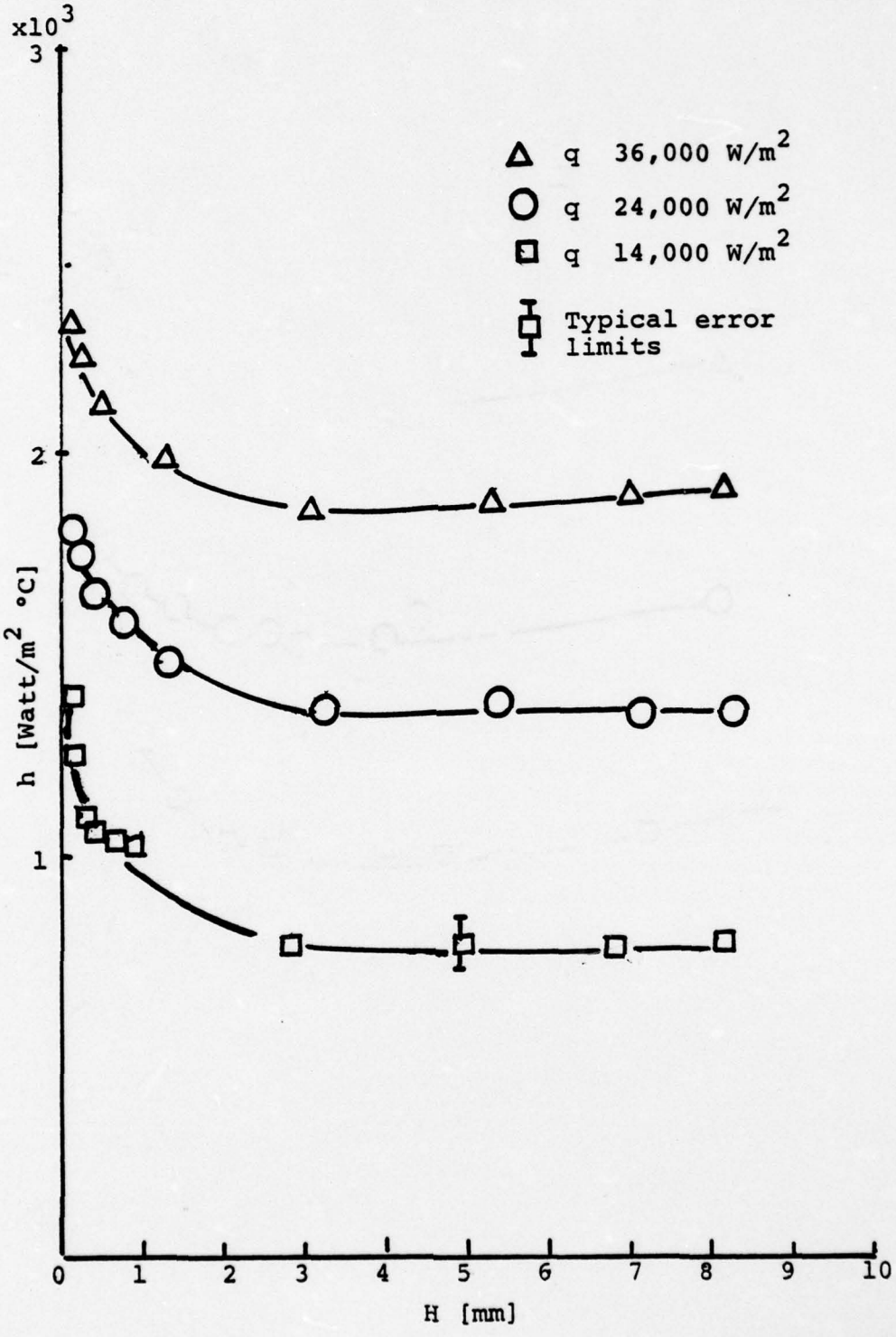

FIGURE 13. Effect of Liquid Level on Heat Transfer Coefficient for Rough (400 Emery) Titanium Foil

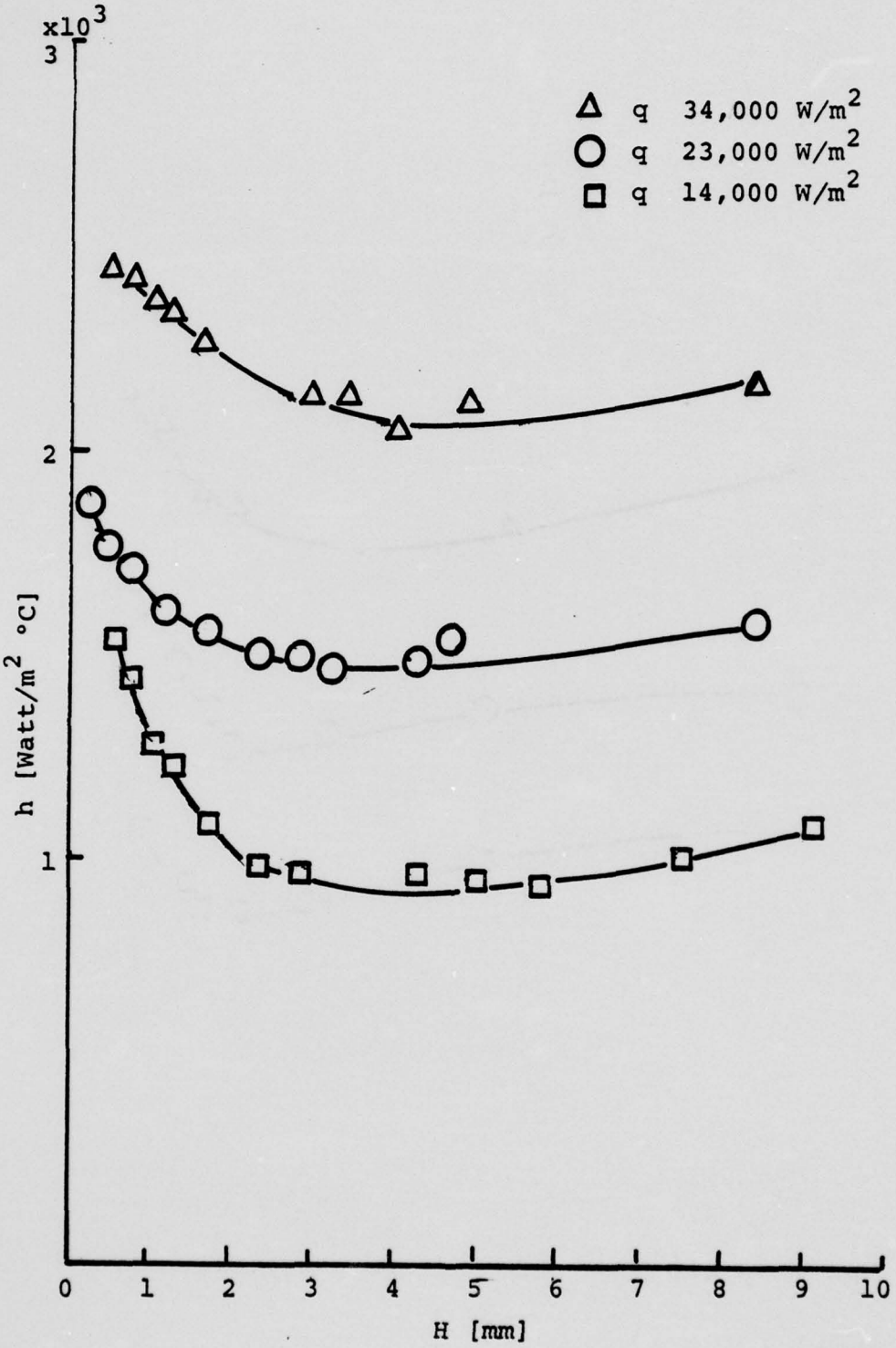

FIGURE 14. Effect of Liquid Level on Heat Transfer Coefficient for Rough (320 Emery) Titanium Foil

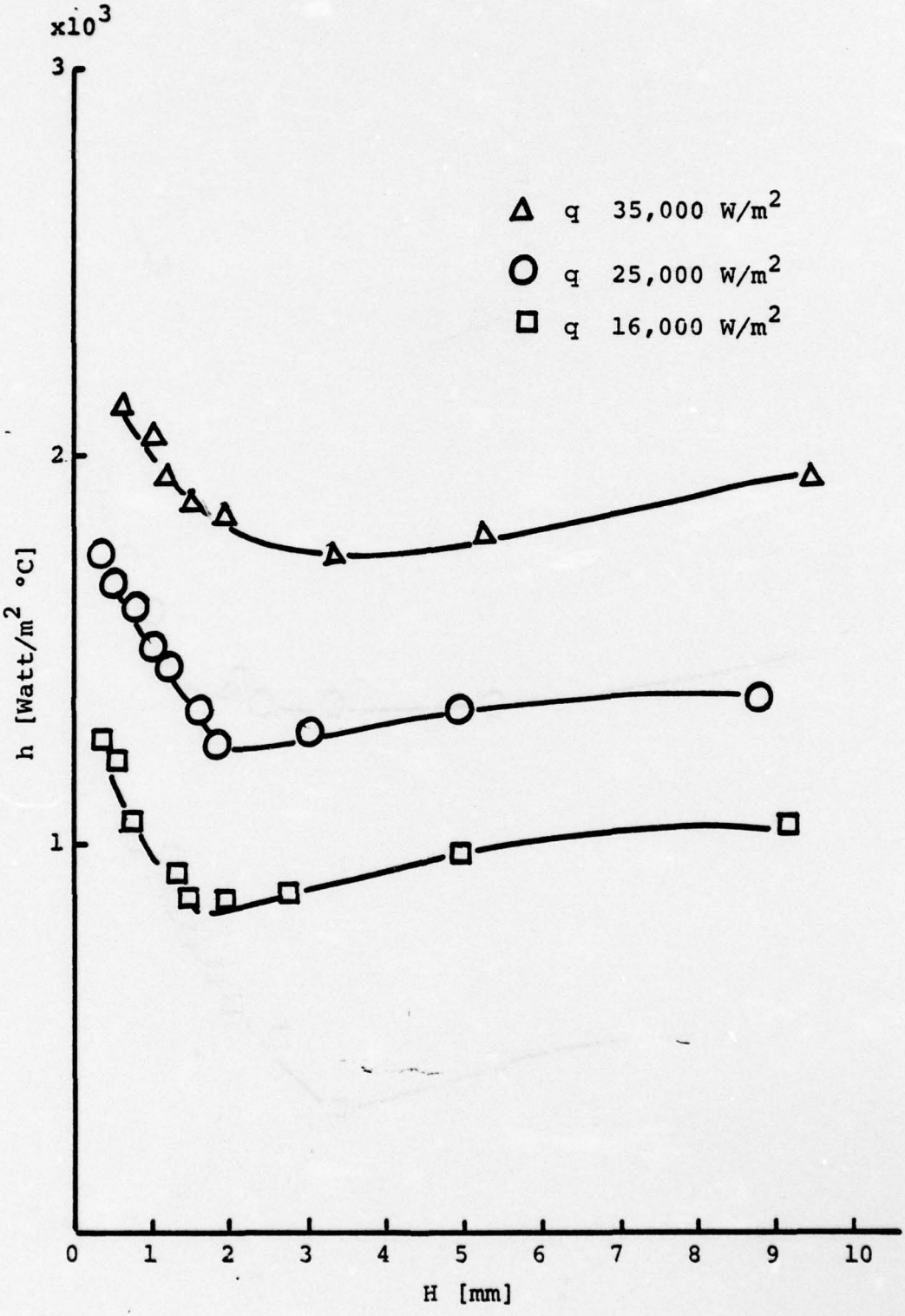

FIGURE 15. Effect of Liquid Level on Heat Transfer Coefficient for Smooth Copper Foil

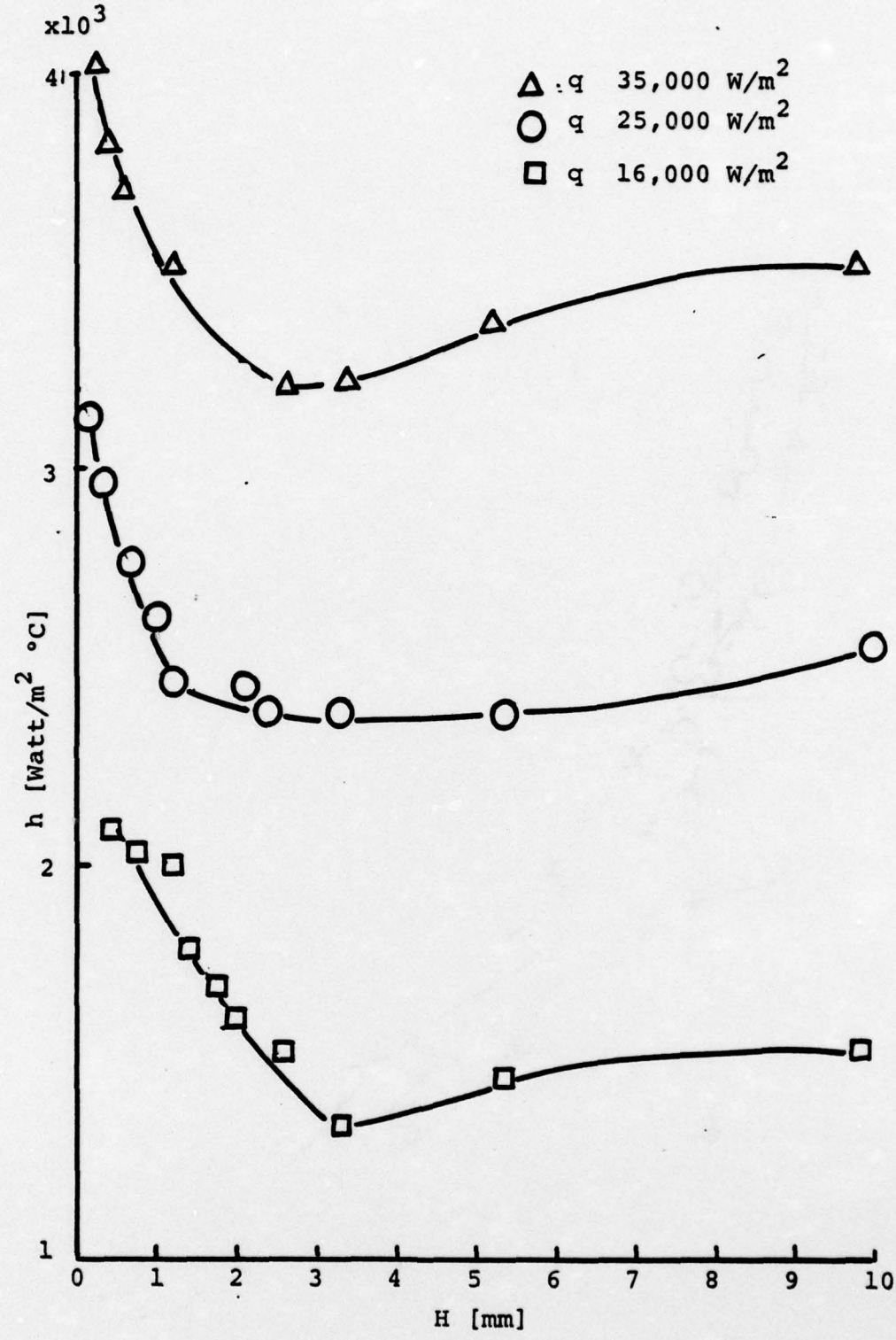

FIGURE 16. Effect of Liquid Level on Heat Transfer Coefficient for Rough (320 Emery) Copper Foil

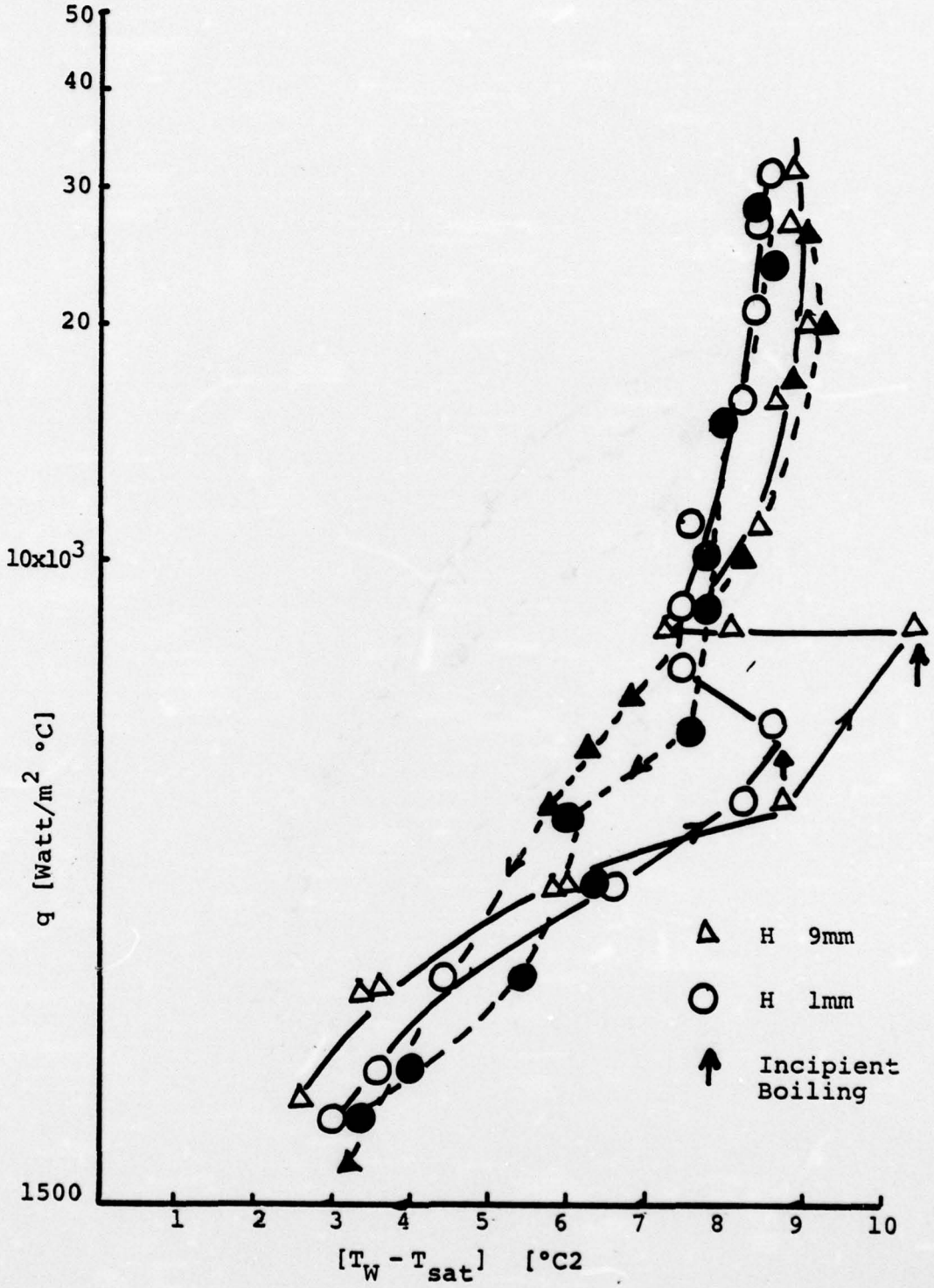

FIGURE 17. Comparison of Incipient Boiling Point for Pool Boiling Versus Boiling in Thin Liquid Films (Rough, 400 Emery, Nickel Iron Foil)

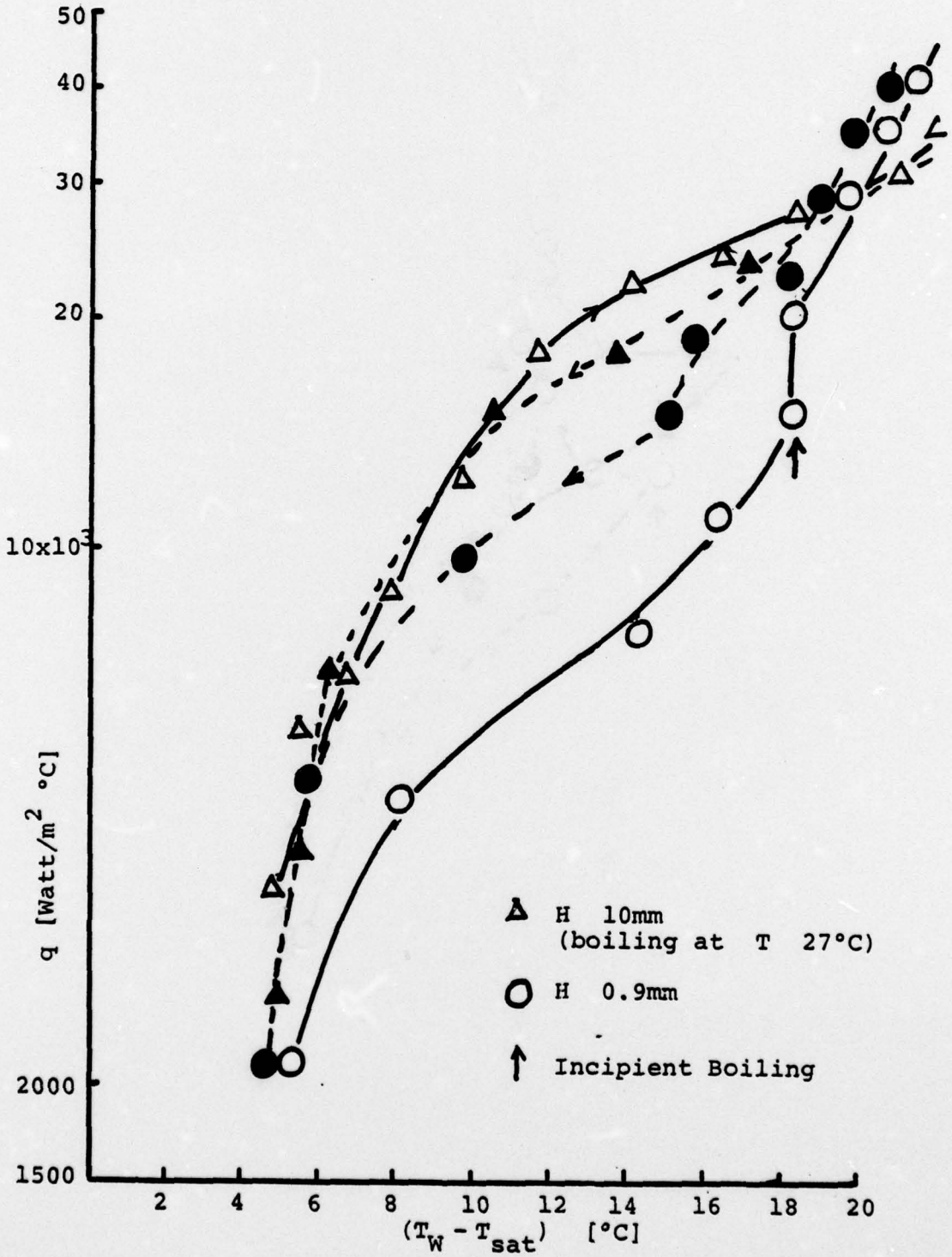

FIGURE 18. Comparison of Incipient Boiling Point for Pool Boiling Versus Boiling in Thin Liquid Films (Smooth, Nickel Foil)

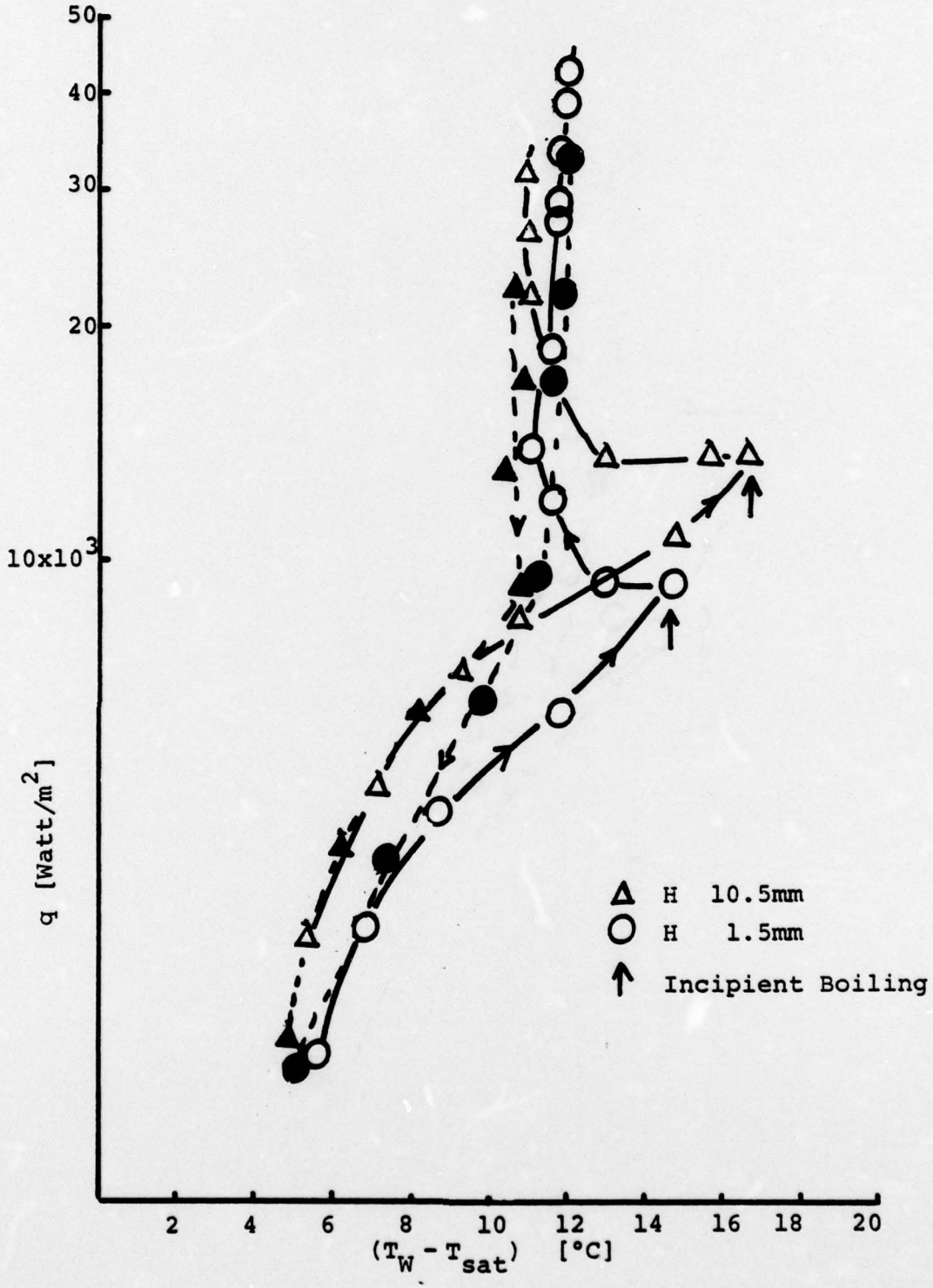

FIGURE 19. Comparison of Incipient Boiling Point for Pool Boiling Versus Boiling in Thin Liquid Films (Rough, 400 Emery, Nickel Foil)

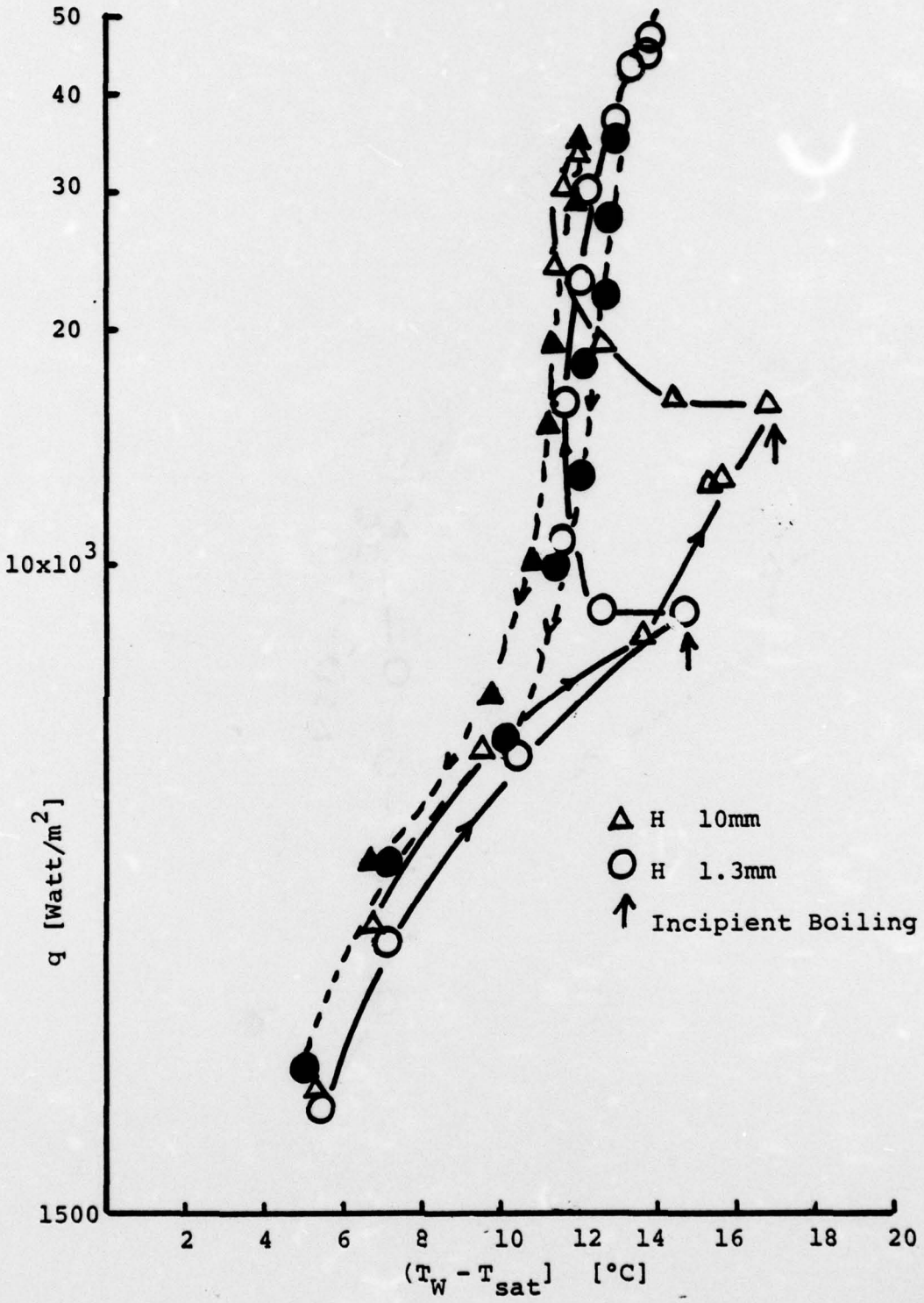

FIGURE 20. Comparison of Incipient Boiling Point for Pool Boiling Versus Boiling in Thin Liquid Films (Rough, 320 Emery, Nickel Foil)

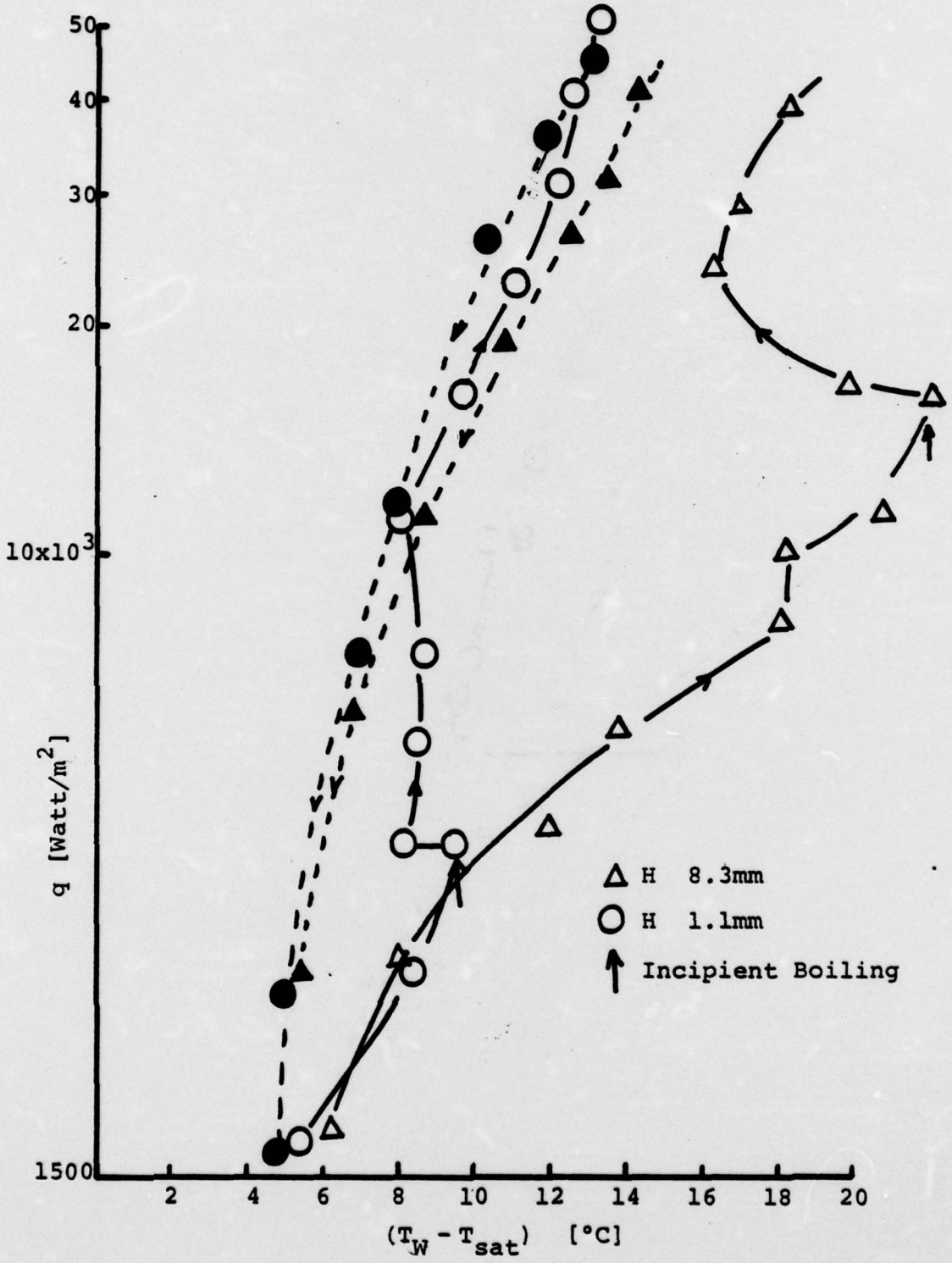

FIGURE 21. Comparison of Incipient Boiling Point for Pool Boiling Versus Boiling in Thin Liquid Films (Smooth, Titanium Foil)

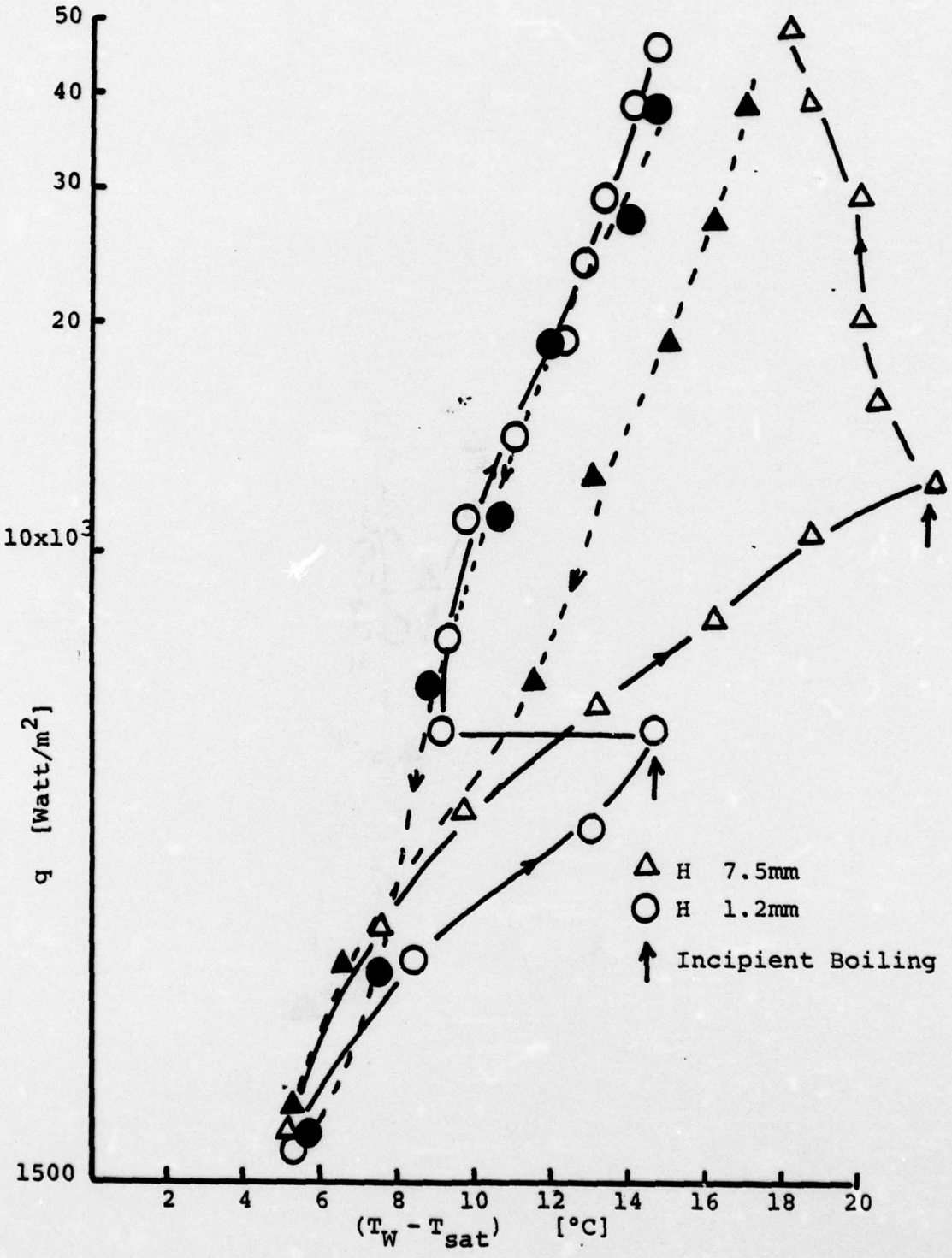

FIGURE 22. Comparison of Incipient Boiling Point for Pool Boiling Versus Boiling in Thin Liquid Films (Rough, 400 Emery, Titanium Foil)

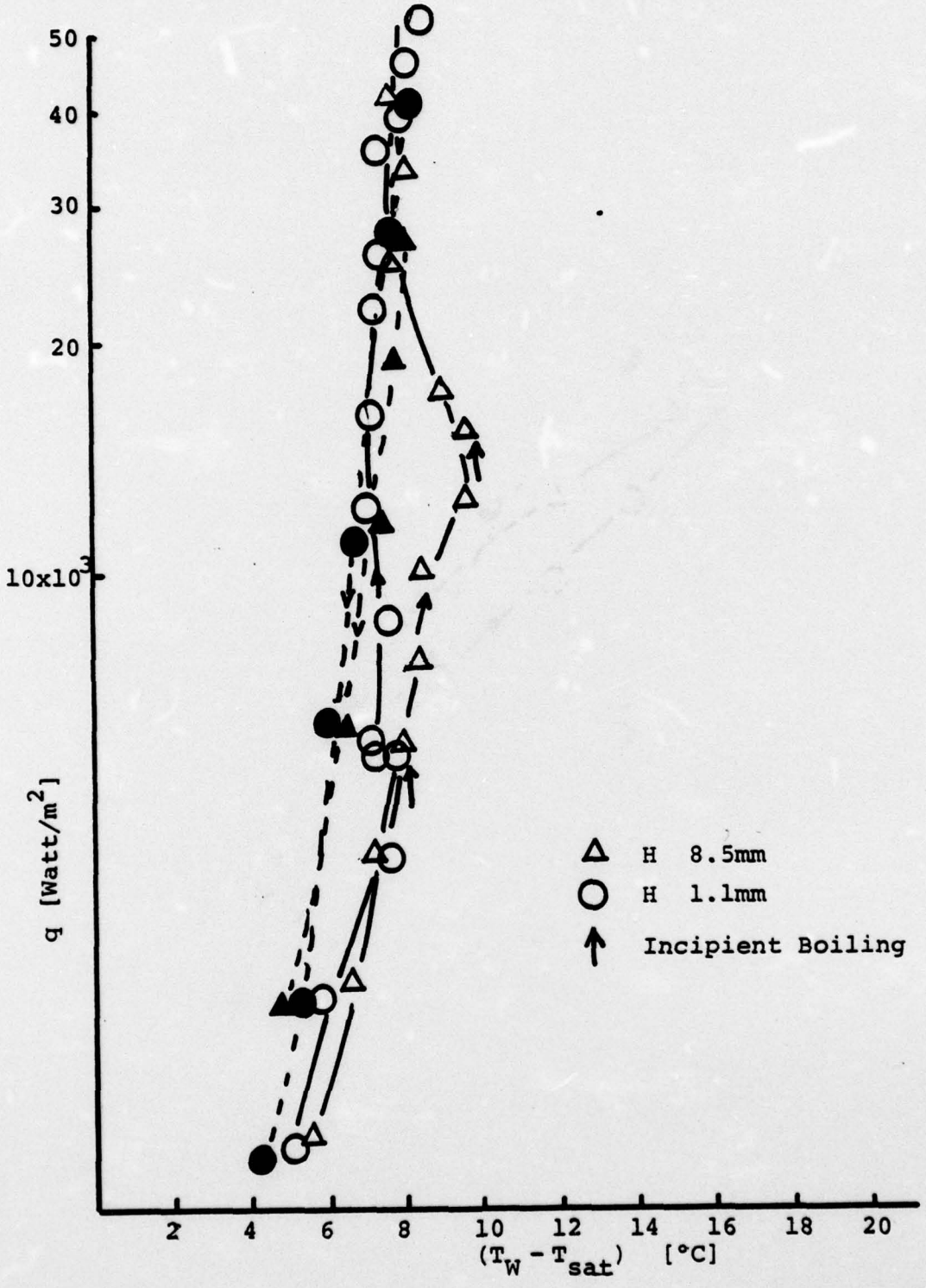

FIGURE 23. Comparison of Incipient Boiling Point for Pool Boiling Versus Boiling in Thin Liquid Films (Rough, 320 Emery, Titanium Foil)

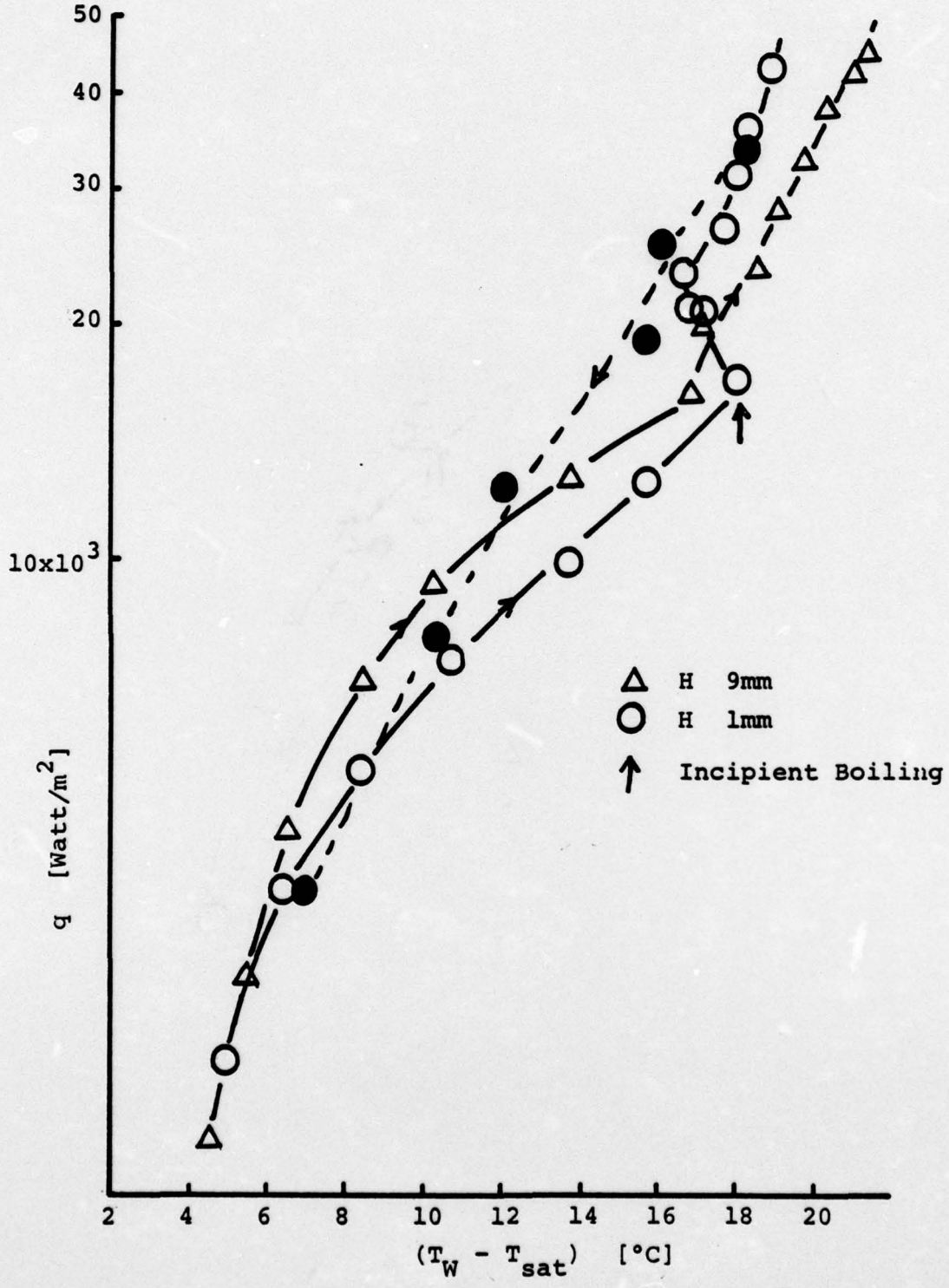

FIGURE 24. Comparison of Incipient Boiling Point for Pool Boiling Versus Boiling in Thin Liquid Films (Smooth, Copper Foil)

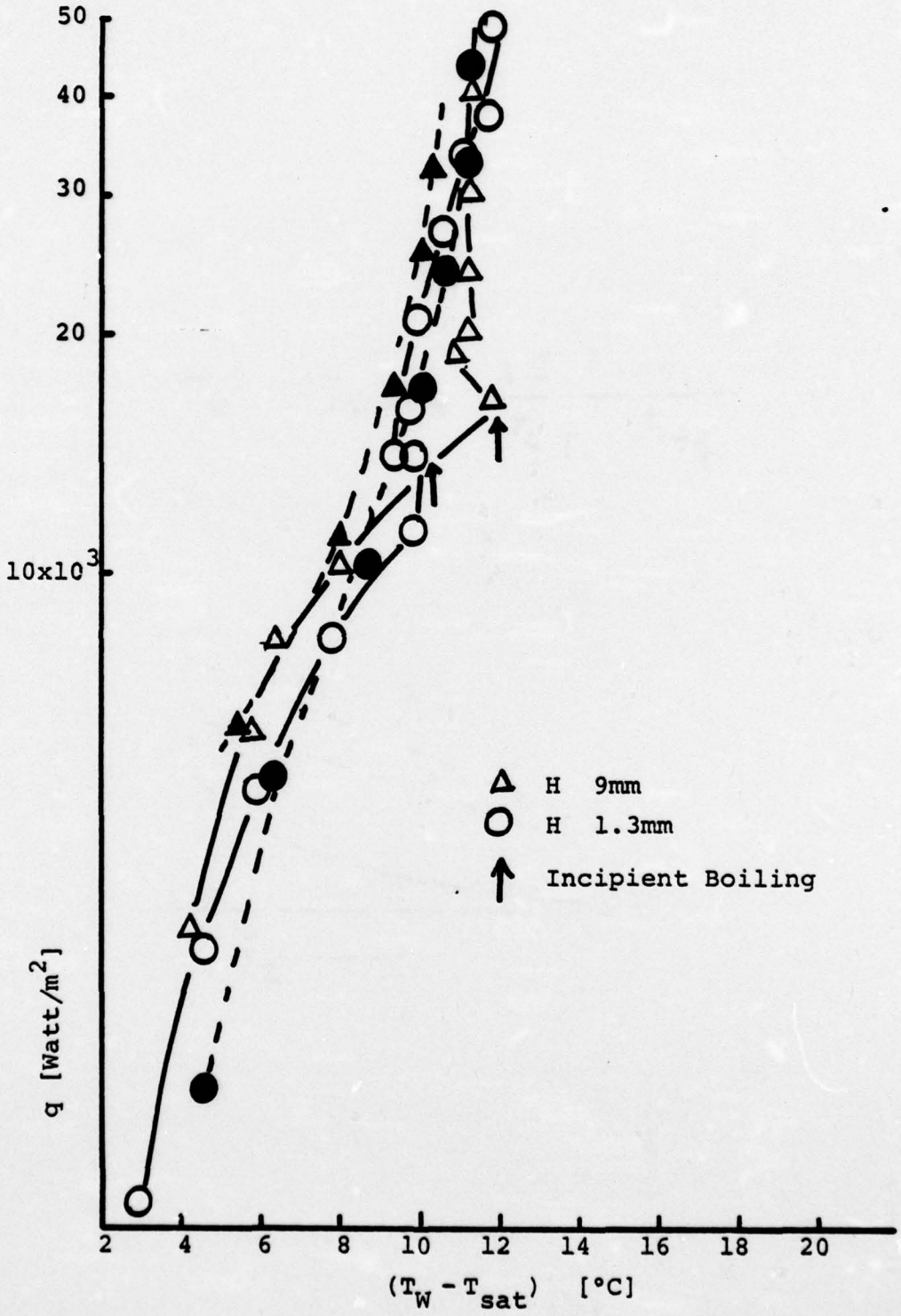

FIGURE 25. Comparison of Incipient Boiling Point for Pool Boiling Versus Boiling in Thin Liquid Films (Rough, 320 Emery, Copper Foil)

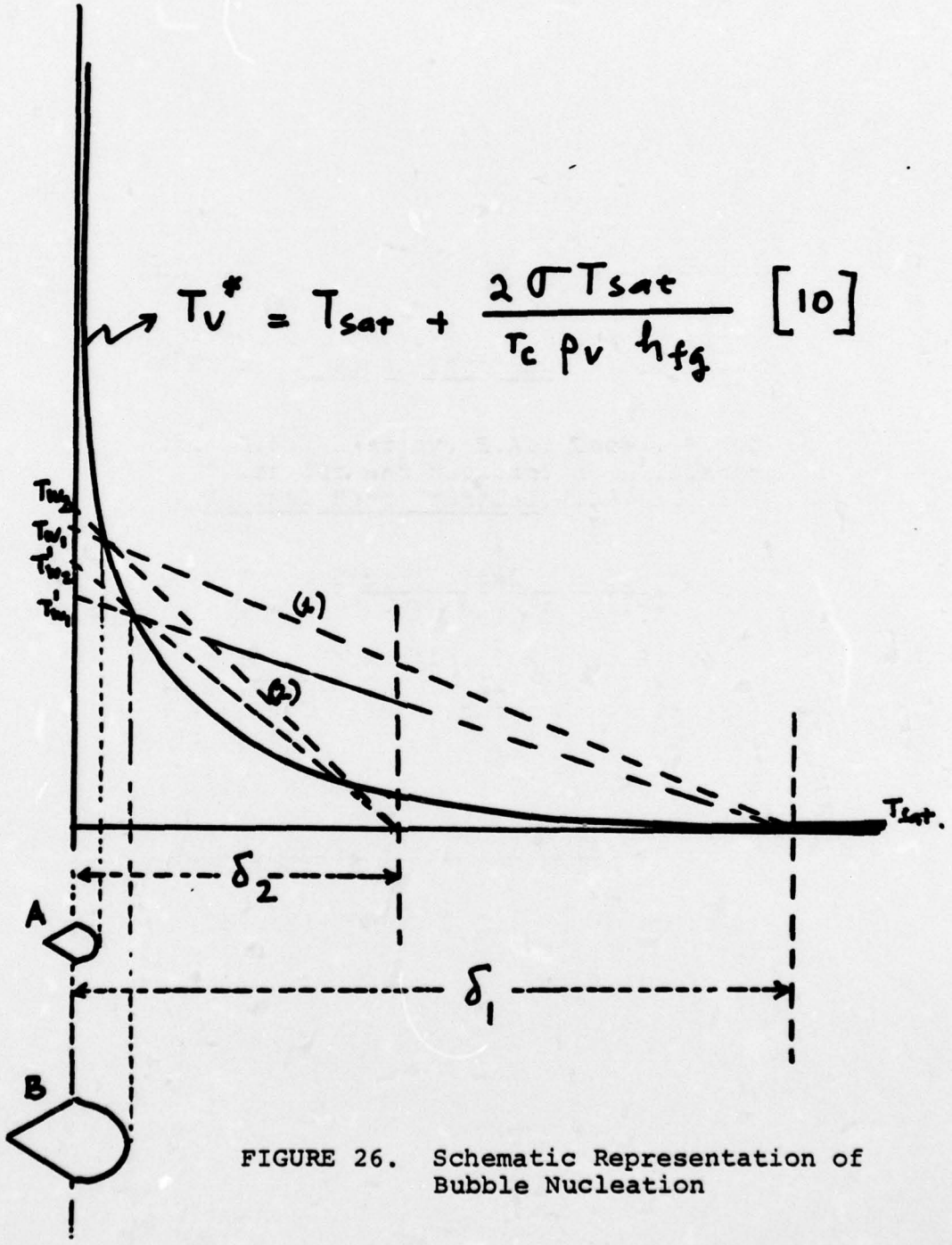

FIGURE 26. Schematic Representation of Bubble Nucleation

LIST OF REFERENCES

1. Bergles, A.E. and Rohsenow, W.M., "The Determination of Force Convection Surface Boiling Heat Transfer," Journal of Heat Transfer, V. 86, No. 3, Page 365-372, 1964.

2. Chapman, R.H., "Saturated Pool and Flow Boiling Studies with Freon 113 and Water at Atmospheric Pressure," Oak Ridge National Lab, Page 219, 1974.

3. Cooper, T.E., Field, R.J. and Meyer, J.F., "Liquid Crystal Thermography and its Application to Study of Convective Heat Transfer," Journal of Heat Transfer, V. 97, No. 3, Page 442-450, 1975.

4. Grigor'ev, Dud Kevich, "Boiliing Cryogenic Liquid in a Thin Film," Thermal Engineer, V. 17, No. 12, Page 74, 1970.

5. Hewitt, G.F., Kearsey, H.A., Lacey, P.M.C. and Pulling, D.J., "Burn Out and Nucleation in Climbing Film Flow," Ints. Journal Heat Transfer,V. 8, No. 5, page 793-814, 1965.

6. Holman, J.P., Experimental Methods for Engineers, McGraw-Hill Book Company, Page 37-40, 1966.

7. Marto, P.J., MacKenzie, D.K. and Rivers, A.D., "Nucleate Boiling in Thin Liquid Films," AICHE Paper No. 16, 16th National Heat Transfer Conference, St. Louis, August 1976.

8. Nishikawa, H., Kusuda, K., Yamasaki and K. Tanaka, "Nucleate Boiling at Low Liquid Levels," Trans. Japan Society of Mechanical Engineers, V. 10, No. 38, Page 328-338, 1967.

9. Raad, T., and Myers, J.E., "Nucleation Studies in Pool Boiling on Thin Plates using Liquid Crystals," American Institute of Chemical Engineers Journal, V. 17, No. 5, Page 1260-1261, 1971.

10. Ronshenow, W.M. and Cho, H., "Heat, Mass and Momentum Transfer," International Series in Engineering, 1961.

11. Scott, A.W., Cooling of Electric Equipment, John Wiley and Son, N.Y., Page 251-253, 1974.

12. Yih-Yun, Hsu and Graham, R.W., "Transport Process in Boiling and Two Systems," Series in Thermal and Fluid Engineering, Page 5-12, 1976.

13. Zuber, N. and Staub, F.W., "Stability of Dry Patch Forming in Liquid Film Flowing over Heated Surfaces," Inst. J. Heat Mass Transfer, V. 9, No. 9, Page 897-905, 1966.

INITIAL DISTRIBUTION LIST

		No. Copies
1.	Defense Documentation Center Cameron Station Alexandria, Virginia 22314	2
2.	Library, Code 0212 Naval Postgraduate School Monterey, California 93940	2
3.	Department Chairman, Code 69 Department of Mechanical Engineering Naval Postgraduate School Monterey, California 93940	1
4.	Professor Paul J. Marto, Code 69Mx Department of Mechanical Engineering Naval Postgraduate School Monterey, California 93940	1
5.	LCDR Soehana, Indonesian Navy Jl. Saliman 3 Komplex Al. Kenjeran Surabaya, Indonesia	1